UNIVERSITY OF OSLO
Department of Geosciences
MetOs section

Implementation and evaluation of a parametrization of coarse nitrate

Master thesis in Geosciences Meteorology and Oceanography

Haldis Berge

24th August 2009

Abstract

Aerosols have in recent years been given increased attention due to their effects on climate and health. Drastic reductions in sulphur emissions in Europe during the last two decades have led to a larger relative importance of nitrate aerosols. However, large uncertainties still exist in the representation of nitrate in atmospheric models.

In this thesis heterogeneous reactions of HNO_3 on dust and sea-salt, representing a major pathway of nitrate formation, have been implemented in the Unified EMEP model. A kinetic approach has been used assuming a total reaction in the direction towards nitrate. The aim of this thesis has been to investigate whether reactions of HNO_3 on dust and sea-salt can improve the Unified EMEP model's performance in terms of nitrate compounds. A stepwise approach has been chosen to implement the different processes and reaction sites one after another.

In June 2006 and January 2007 two intensive measurement campaigns where conducted, which separated coarse and fine nitrate. In this thesis, the results of the new nitrate implementation have been evaluated in detail against these and other measurements within the EMEP network, showing that the temporal correlation of coarse nitrate has clearly improved. However, it has also been found that the implementation yields too small values of coarse nitrate over land. This negative bias will be an important issue for future work.

Acknowledgement

First of all I would like to thank my supervisor Hilde Fagerli for all help and guidance throughout this thesis. Thanks for being so patient and giving me an introduction to the Unified EMEP model. I am very grateful to Svetlana Tsyro for helping me to understand sea-salt and dust emissions and parametrizations in the Unified EMEP model. Their assistance and feedback are highly appreciated. Thanks go to Frode Stordal for being my co-supervisor.

The participating partners to the EMEP intensive measurement periods are greatly acknowledged for sharing their data. Thanks to Wenche Aas and Anne Gunn Hjellbrekke at NILU for answering all my questions about the measurements data. Thanks to Heiko Klein who has made the plotting tools of the scatterplot and timeseries used in this thesis. I would also like to thank Àlvaro M. Valdebenito, Seemena Valiyaveetil and Agnes Nyiri. I am also grateful of all matlab help Silje Sørland has given me. Thank to Gunnar Wollan for helping out with computer problems.

And last but not least I want to thank the girls at the study hall for keeping my spirit up and all their support through the study. I am very grateful to Anne Solveig for proof reading.

Contents

Chapter 1

Introduction

Due to extensive control measures, sulphur emissions have been reduced drastically in large parts of Europe and North America after the 1970s. Also emissions of nitrogen oxides and ammonia have decreased, albeit not as much. Due to the chemical interaction between sulphur and nitrogen compounds in the atmosphere, the large reduction of sulphur emissions has offset the decrease in nitrate aerosols and in some cases even led to a slight increase. The relative importance of nitrate aerosols with respect to other aeorsols has thus increased. Over Europe nitrate aerosols now account for 10-20% of the total dry aerosol mass (Putaud et al., 2004) and affect the ecosystem through acidification and eutrophication. They also have adverse effects on human health and contribute to climate change.

Inorganic aerosols such as sulphate, nitrate and ammonium and their precursor gases sulphur dioxide, nitrogen oxides and ammonia cause acidification when deposited to the Earth's surface. Nitrogen species can also act as nutrients. Species adapted to nitrogen deficiency may, when nutrient loads increase, be outcompeted by species with higher nitrogen demand, resulting in a loss of biodiversity (Krupa, 2003).

Aerosols play a role in the degradation of air quality. Health effects related to particulate matter (PM) include asthma, lung cancer, cardiovascular deseases, and premature death. Current exposure to PM from anthropogenic emissions leads to the loss of 8.6 months on average of life expectancy in Europe (WHO,2006).

Nitrate aerosols affect the climate both directly and indirectly. Bauer et al. (2007) studied nitrate aerosols and estimated the present nitrate forcing to be -0.11 W/m^2,

while Myhre et al. (2006) estimated the radiative forcing of nitrate aerosols to be -0.02 W/m^2. In IPCC (2007) the direct radiative forcing of aerosols was calculated to -0.9 W/m^2 $\pm$ 0.4 W/m^2. Martin et al. (2004) found that radiative forcing of nitrate was about 10-15% of the sulphate forcing. Indirect climate effects of nitrate aerosols occur through their influence on the chemistry of ozone, an important climate gas, as heterogeneous chemistry involving nitrate constitutes a sink for nitrogen oxides.

Given the importance of nitrate aerosols, observational and modelling tools have been applied to follow their evolution and to study the chemical and physical processes involved in their formation. The main objective of the EMEP programme (Co-operative programme for monitoring and evaluation of the long-range transmission of air pollutants in Europe) is to provide governments and subsidiary bodies under the Convention on Long-Range Transboundary Air Pollution (LRTAP), signed in 1979, with qualified scientific research to support development and further evaluation of the international protocols on emission reduction negotiated within the Convention. Measurements from the EMEP network and calculations performed with the Unified EMEP model have been important as a basis for a number of emission control protocols (e.g the Gothenburg protocol in 1999). The Unified EMEP model has been developed at the Meteorological Synthesizing Centre - West (MSC-W) at the Norwegian Meteorological Institute, one of the five centres under the EMEP programme.

Nitrate has a relatively complicated chemistry, as it is semi-volatile and enters into a complex chemical equilibrium with sulphuric acid, ammonium, ammonia, nitric acid, sea-salt and mineral dust. In addition, nitrate aerosols are size-distributed, with large aerosols having different physical properties than small aerosols (e.g. large aerosols are subject to faster dry deposition). The size distribution of nitrate can thus be decisive for the model results.

In recent years there have been several model studies of coarse nitrate formation on dust and sea-salt (Hodzic et al., 2006; Myhre et al., 2006; Feng and Penner, 2007; Liao et al., 2003; Bauer et al., 2007; Capaldo et al., 2000). In this thesis a new parameterization of coarse nitrate formation on dust and sea-salt is implemented. The parametrization follows the same method as Hodzic et al. (2006), where a total heterogeneous reaction in the forward direction between HNO_3 and mineral dust is assumed.

Model results, however, have to be evaluated continuously against measurements in order to remain trustworthy. Up to now only limited observations separating HNO_3 and particulate nitrate (NO_3^-) exist for Europe, in particular measurements that separates coarse and fine particles. This is about to change as a result of measurements in the EU-project NitroEurope and campaigns in the EMEP network. In this thesis measurements from the intensive periods in the EMEP monitoring network and standard measurements from the EMEP monitoring network are used to evaluate Unified EMEP model results and the new parametrization of coarse nitrate.

The thesis will start by describing in chapter 2 the underlying theory with focus on nitrogen compounds and their precursors. Chapter 3 will review some of the main features of the Unified EMEP model, followed by a detailed description of all the new implementations and sensitivity tests performed for this thesis. In chapter 4 the new parametrization will be discussed and evaluated in detail. Finally, summary and conclusions are given in chapter 5.

Chapter 2

Background

In this chapter, atmospheric processes and chemistry of relevance for nitrogen oxides (NO_x=NO + NO_2) are described, followed by a description of the formation of nitrate aerosols. Different sources of nitrate aerosol precursors will be presented.

2.1 Atmospheric processes

The theoretical description given in this section is based on Pandis and Seinfeld (1998) and Jacob (1999). The atmosphere's chemical composition is mainly controlled by four types of processes:

- *Emissions.* Chemical species are emitted to the atmosphere by anthropogenic and natural emissions. Natural emissions can be subdivided into biogenic and non-biogenic emissions.

- *Chemistry.* Chemical reactions lead to the production and loss of chemical species.

- *Transport.* The gases and aerosols in the atmosphere are transported from their sources by advection, turbulence and convection.

- *Deposition.* There are two types of deposition; dry deposition (i.e. direct reaction or absorption on the ground) and wet deposition (scavenging by precipitation).

Numerical models are used to simulate these processes on computers. Models that divide the atmosphere into grid boxes are called Eulerian models. In this kind of models, the rate of change of the abundance of a species X over time inside one grid box must equal the sum of all sources and sinks of the species within the grid box. This rate of change in concentration c of species X can be expressed as:

$$\frac{dc}{dt} = \sum \text{sources} - \sum \text{sinks} = \mathrm{F_{in}} + \mathrm{E} + \mathrm{P} - \mathrm{F_{out}} - \mathrm{L} - \mathrm{D} \tag{2.1}$$

where F_{in} and F_{out} are the transport into and out of the grid box, respectively, E is the emission of species X, P is the chemical production, L is the chemical loss and D is the deposition of species X within the grid box.

The atmospheric lifetime τ is a measure of how long it takes for a species to diminish by a factor 1/e, thus called e-folding lifetime. It is a useful measure of the time it takes for a system to reach steady state, and can be calculated as follows:

$$\tau = \frac{\mathrm{c}}{\sum \text{sinks}} = \frac{\mathrm{c}}{\mathrm{F_{out}} + \mathrm{L} + \mathrm{D}} = \frac{1}{\mathrm{k}} \tag{2.2}$$

where k is the overall rate coefficient of the loss processes. Species with short lifetimes will be present in high concentrations around their sources, and in low concentrations far away from their sources. Species with very long lifetimes on the other hand will be more uniformly distributed.

2.2 Atmospheric chemistry of nitrate

The oxidizing capacity of the atmosphere is of key importance for atmospheric chemistry, a major oxidant being the OH radical. The OH radical is produced when solar UV radiation decomposes ozone (O_3) into molecular oxygen (O_2) and energetically excited oxygen atom ($O^1(D)$):

$$\mathrm{O_3} + \mathrm{hv} \longrightarrow \mathrm{O_2} + \mathrm{O}^1(\mathrm{D}) \tag{2.3}$$

$$\mathrm{O}^1(\mathrm{D}) + \mathrm{H_2O} \longrightarrow 2\,\mathrm{OH} \tag{2.4}$$

The main sinks of OH are carbon monoxide (CO) and methane (CH_4), and the resulting lifetime of OH is on the order of one second. This short lifetime causes highly variable OH concentrations, with OH responding rapidly to changes in sources and sinks. As the formation of OH requires sunlight it exists only during daytime. For tropospheric chemistry all the cycles involving CO, CH_4, O_3

and NO_x are of key importance. However, only the NO_x cycle will be described here since this is the most important cycle for the understanding of aerosol nitrate formation.

2.2.1 The NO_x cycle

NO_x is mainly emitted as NO, but during daytime NO rapidly establishes (on a timescale of minutes) an equilibrium with NO_2 in the null cycle:

$$NO + O_3 \longrightarrow NO_2 + O_2 \tag{2.5}$$

$$NO_2 + hv \xrightarrow{O_2} NO + O_3 \tag{2.6}$$

This rapid cycling makes it most appropriate to consider the budget of NO_x as a whole. At night NO_x is present as NO_2 as there is no photolysis at night. The principal sink of NO_x during daytime is oxidation to HNO_3:

$$NO_2 + OH + M \longrightarrow HNO_3 + M \tag{2.7}$$

were M represents an inert molecule that absorbs excess molecular energies. However, as OH requires sunlight, reaction 2.7 does not occur during night time. At night time the sink of NO_x is oxidation of NO_2 by O_3:

$$NO_2 + O_3 \longrightarrow NO_3 + O_2 \tag{2.8}$$

$$NO_3 + NO_2 + M \longrightarrow N_2O_5 + M \tag{2.9}$$

$$N_2O_5 + H_2O \xrightarrow{\text{aerosol}} 2\,HNO_3 \tag{2.10}$$

This sink is not efficient during daytime as the NO_3 radical is rapidly photodissociated back into NO_x:

$$NO_3 + hv \longrightarrow NO_2 + O \tag{2.11}$$

$$NO_3 + hv \longrightarrow NO + O_2 \tag{2.12}$$

Overall NO_x has a lifetime of approximately one day. HNO_3 is highly soluble in water and thus scavenged by precipitation, an additional sink for HNO_3 are reactions with sea-salt and dust. The lifetime of HNO_3 is on the order of a few days in the lower troposphere due to wet and dry deposition. This short lifetime makes HNO_3 an insufficient reservoir for NO_x.However, PAN (peroxyacetyl nitrate) which is formed from carbonyl compounds, can act as a reservoir for NO_x. Especially at low temperatures PAN is rather stable and can be transported over long distances.

2.2.2 Nitrate aerosols

The atmosphere contains significant concentrations of aerosol particles, both in urban and remote areas. Aerosols stem from direct emissions (primary aerosols) and from gas-to-particle conversion (secondary aerosols). Aerosols are generally considered to be particles in the size range from a few nanometers (nm) to tens of micrometers (μm) in diameter. They are divided into fine and coarse aerosols, where fine aerosols here are defined to have a diameter (d) of less than 2.5 μm ($PM_{2.5}$) and the coarse fraction has a diameter larger than 2.5 μm. In the fine fraction the aerosols are mostly from condensation of precursors gases. The fine mode is often further divided into a nucleation mode, ranging from $\sim$ 0.005 to 0.1 μm in diameter and an accumulation mode from 0.1 to 2.5 μm. From mechanical action of the wind at the Earth's surface sea-salt, soil dust, and vegetation debris are emitted into the atmosphere. These aerosols exist mainly in the size range from 1 to 10 μm. Finer aerosols are difficult to generate mechanically because of their large area-to-volume ratios and hence high surface tension per unit aerosol volume, while coarser aerosols are not easily lifted by the wind and they have short atmospheric lifetimes due to efficient sedimentation. There are two removal processes of atmospheric aerosols: deposition at the Earth's surface (dry deposition) and incorporation into cloud droplets during the formation of precipitation (wet deposition). The bulk of atmospheric aerosols are found in the lower troposphere and their lifetimes are on the order of 1-2 weeks.

Nitrate aerosol is one of the major compounds of the suspended particulate matter in the atmosphere. It represents between 5-15% of the total aerosol particulate mass smaller than 10 μm diameter (PM_{10}) (Hodzic et al., 2006). Most of the nitrate mass is found in the fine aerosol fraction.

Fine nitrate formation

Fine nitrate consists mainly of ammonium nitrate (NH_4NO_3) which is formed through reactions between ammonia and nitric acid. Formation of ammonium nitrate proceeds in areas of high ammonia and nitric acid concentrations, when sulphuric acid (H_2SO_4) concentrations are low. Nitric acid competes with sulphate to react with the available ammonium. First, sulphuric acid and ammonium react through reaction 2.13, and the excess ammonium then reacts with nitric acid through reaction 2.14.

$$2\,\mathrm{NH_3(g)} + \mathrm{H_2SO_4(a)} \longrightarrow \mathrm{(NH_4)_2SO_4(s)} \tag{2.13}$$

$$\mathrm{NH_3(g) + HNO_3(g) \rightleftharpoons NH_4NO_3(a,s)} \tag{2.14}$$

where g indicates the gaseous phase of the species, a the aqueous phase and s the solid phase. Ammonium nitrate can exist as a solid or in aqueous solution of NH_4^+ and NO_3^- depending on the ambient relative humidity (RH). If RH is less than the deliquescence relative humidity (DRH) ammonium nitrate is a solid. The DRH is dependent on temperature (Pandis and Seinfeld, 1998):

$$\ln(\mathrm{DRH}) = \frac{723.7}{\mathrm{T}} + 1\,.6954 \tag{2.15}$$

were T is the temperature in kelvin. Higher formation of solid ammonium nitrate thus occurs at low temperatures, which gives rise to a seasonal variation with higher ammonium nitrate formation in winter.

Coarse nitrate formation

Coarse nitrate is associated with sea-salt and crustal elements in dust (Wu and Okada, 1994). In marine areas with high sodium concentrations HNO_3 produces sodium nitrate ($NaNO_3$) and in areas with crustal material from local soil or desert dust HNO_3 produces calcium nitrate ($Ca(NO_3)_2$) and magnesium nitrate ($Mg(NO_3)_2$) (Mamane and Gottlieb, 1992; Krueger et al., 2004) through the following reactions:

$$\mathrm{HNO_3(g) + NaCl(s,a) \longrightarrow NaNO_3(a) + HCl(g)} \tag{2.16}$$

$$\mathrm{2\,HNO_3(g) + CaCO_3(s) \longrightarrow Ca(NO_3)_2(s) + CO_2(g) + H_2O(l)} \tag{2.17}$$

where l indicates the liquid phase. Calcite ($CaCO_3$) and dolomite ($MgCa(CO_3)_2$) constitute the most reactive part of dust towards HNO_3 (Usher et al., 2003; Krueger et al., 2004; Vlasenko et al., 2006).

Reaction 2.14 will reach equilibrium within a few seconds (Capaldo et al., 2000) while the timescale for coarse nitrate to reach equilibrium is on the order of hours (Meng and Seinfeld, 1996). Ammonium sulphate forms first as this reaction is faster than the formation of ammonium nitrate. If there is any excess NH_3 ammonium nitrate forms. Any excess of HNO_3 present after this equilibrium has been reached, will react with dust and/or sea-salt to form coarse nitrate.

2.3 Sources of nitrate precursors

The most abundant precursors of aerosol nitrate are ammonia and nitric acid. In this section the sources of NH_3 and HNO_3, their geographical distribution and lifetimes will be described. In addition a short description of sources of dust and sea-salt and their geographical variation will be given.

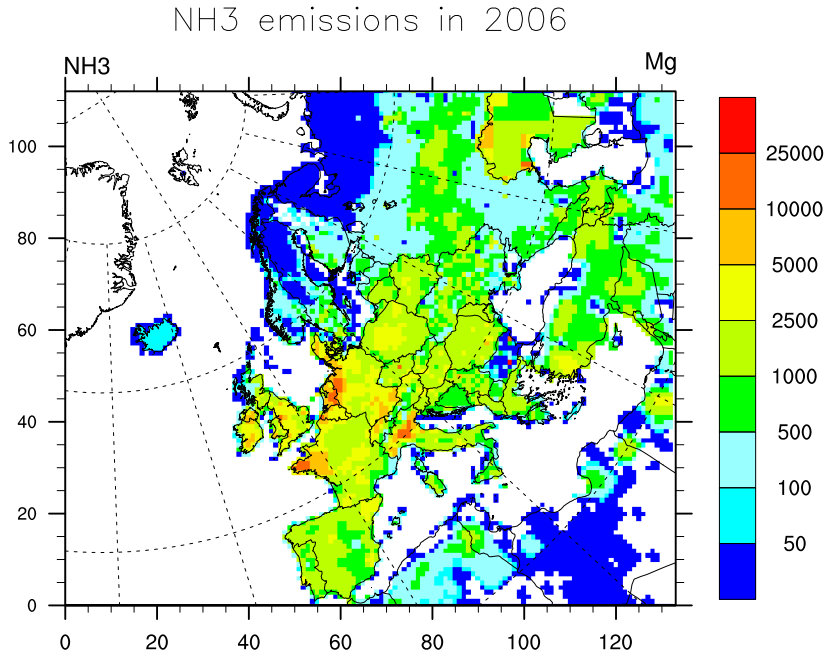

Figure 2.1: *Emissions of NH_3 used for 2006 in the Unified EMEP model in Mg. NH_3 reflects the largest agricultural areas in Europe. Data from CEIP (Centre on Emission Inventories and Projections).*

Agricultural emissions in the form of animal waste represent the main source of ammonia to the atmosphere. Fertilizing, soil processes and industrial activity also contribute to NH_3 emissions. The primary removal mechanism of NH_3 involves the conversion to ammonium-covered aerosols as ammonium sulphate and ammonium nitrate, which are deposited to the ground by wet and dry deposition. This gives an atmospheric lifetime of NH_3 of 1 - 5 days, and NH_3 will only be transported over short distances from its sources. The spatial distribution of NH_3 emissions used in this study for the year 2006 is shown in Figure 2.1.

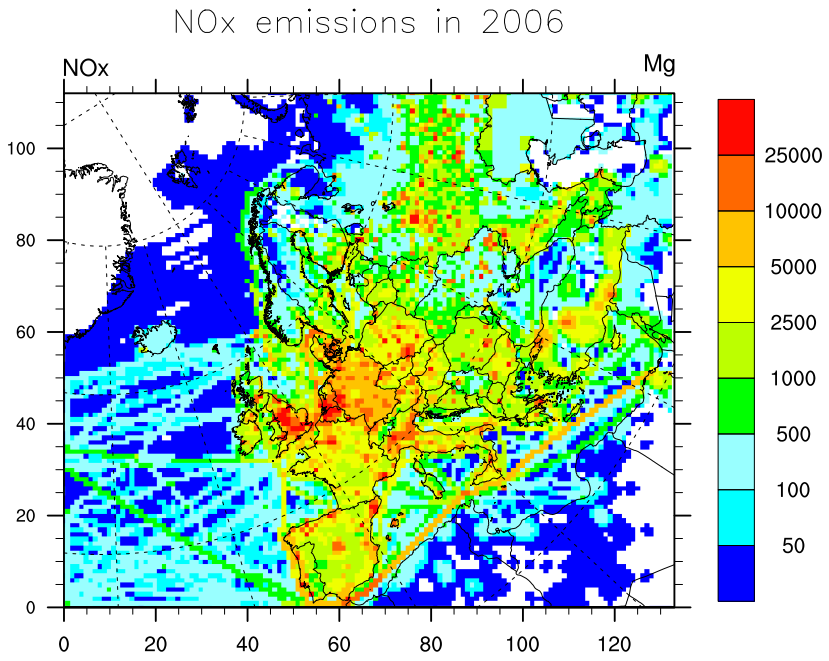

Figure 2.2: *Emissions of NO_x used for 2006 in the Unified EMEP model in Mg. NO_x clearly reflect ship tracks. Data from CEIP (Centre on Emission Inventories and Projections).*

HNO_3 forms from NO_x as described in the previous section. Anthropogenic NO_x emissions in Europe are dominated by fossil fuel combustion in road traffic, with a 40% share in 2005, followed by power plants (22%), industry (16%), off-road transport (15%) and the residential sector (7%) (Vestreng et al., 2009, and references therein). Other minor sources of NO_x in the troposphere are natural sources such as lightning, soil, oxidation of NH_3 emitted from the biosphere and downward transport of nitrogen from the stratosphere. NO_x has a lifetime of only about one day in the lower troposphere and thus is transported over even shorter distances than NH_3. In Figure 2.2 the NO_x emissions used in this study for the year 2006 are shown.

One of the main sources of atmospheric aerosols is the ocean with emissions of $\sim$ 1000 to 5000 Tg per year (Wallace and Hobbs, 2006). The main mechanism of

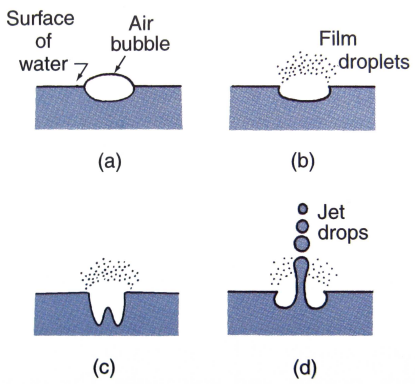

Figure 2.3: *Schematics of the formation of film- and jet-droplets when an air bubble burst at the surface of water. From Wallace and Hobbs (2006).*

ejecting sea material into air is bubble bursting. An additional source is material that is torn from windblown sea spray and foam (giant sea-salt aerosols). These giant sea-salt aerosols are large and their lifetime is relatively short. Film- and jet-droplets are produced from bubble bursting. Film-droplets are made when an air bubble's film breaks at the sea surface (Figure 2.3b). An air bubble ≥ 2 μm in diameter can give $\sim$ 100 to 200 film-droplets. After evaporation these film-droplets will become sea-salt aerosols with diameter less than 0.3 μm. Up to five jet-droplets break away from each jet that forms after a bubble burst (Figure 2.3d). These jet-droplets are thrown into the air and some of them evaporate and give sea-salt aerosols with diameters larger than 2 μm. Estimates of sea-salt emissions per year are given in Table 2.1.

Dust emissions originate predominantly from arid and semiarid environments, which account for $\sim$ 33% of the global land area. They provide $\sim$ 2000 Tg per year of mineral particles (Wallace and Hobbs, 2006). Most dust storms occur in the region starting at the west coast of Northern Africa extending east through the Middle East into Central Asia. This dust can be transported over large distances through long-range global transport. This transport often occurs in horizontally layered plumes and can persist for days to a week over thousands of kilometers. Saharan dust has been transported in westerly, northerly, and easterly direction to South America, Northern Europe and the Middle East, respectively (Usher et al. (2003); Husar (2004)). The transfer of dust particles from the Earth's surface to the atmosphere, called sandblasting, is caused by wind and atmospheric tur-

	Northern hemisphere	Southern hemisphere
Sea-salt		
< 1 μm	23	31
1-16 μm	1420	1870
Total	1440	1901
Mineral (soil) dust		
< 1 μm	90	17
1-2 μm	240	50
2-20 μm	1470	282
Total	1800	349

Table 2.1: *Estimates (in Tg per year) for the year 2000 of emissions of sea-salt and dust into the atmosphere, values from IPCC,2001, table 5.3*

bulence. To start the motion of particles at the Earth's surface the surface wind (friction velocity) must exceed a certain threshold value, which is dependent on the surface type and the particle size. For a particle in the size range 50 to 200 μm and for soils containing 50% clay or tilled soil a friction velocity of $\sim$ 0.2 m s^{-1} is required, translating into a wind speed of several meters per second a few meters above the surface. A major source of smaller particles ($\sim$ 10 to 100 μm in diameter) is saltation. Larger sand grains are thrown up into the air, fly a few meters and when they hit the ground they make a burst of dust particles.

Chapter 3

Methodology

In this thesis a special version of the eulerian Unified EMEP Model is used, which includes dust (version rv3_1 hereafter referred to as 'EMEP model'). The following section will briefly describe the EMEP model as it was before the modifications of this master thesis were implemented. The focus will be on model features and routines that are relevant for the formation of nitrate. The model runs performed in this thesis are described in section 3.2. Finally section 3.3 will describe the measurement data used in this thesis.

3.1 The Unified EMEP Model

The EMEP model is a further development from earlier EMEP models described in Berge and Jakobsen (1998), Jonson et al. (1999) and Simpson (1995). For a full documentation see Simpson et al. (2003) and Fagerli et al. (2004). Version rv3_1 is, at the time of writing, the same code as the one that is available at the EMEP web site as open source.

The EMEP model grid is defined in a polar stereographic projection with a horizontal resolution of 50×50 km^2 in 20 sigma layers from the surface up to approximately 100 hPa. The official EMEP area and the model grid are shown in Figure 3.1. The emission input consists of gridded national emissions of sulphur dioxide (SO_2), nitrogen oxides, ammonia, non-methane volatile organic compounds (NMVOC), carbon monoxide and particulate matter ($PM_{2.5}$, PM_{10}), which are officially reported to the LRTAP Convention. The emissions are provided for ten anthropogenic sectors and one additional sector that mainly consists of natural

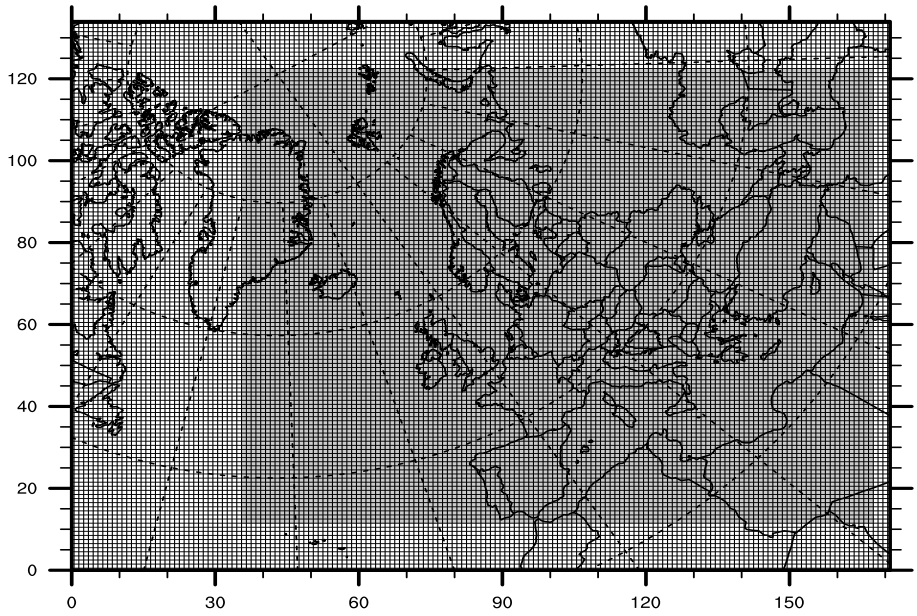

Figure 3.1: *The EMEP model domain, the large area shows the full model domain, the inner area shows the official EMEP grid, from Simpson et al. (2003)*

emissions (Simpson et al., 2003). The emissions are distributed temporally using monthly and daily factors which are specified for each pollutant, emission sector and country. In addition, simple day-night factors are applied for the sectors. The meteorological input is taken from PARLAM-PS (PARallel Limited Area Model with Polar Stereographic map projection), which is a dedicated version of the HIRLAM (HIgh Resolution Limited Area Model) Numerical Weather Prediction Model maintained and verified at the Norwegian Meteorological Institute. The numerical advection scheme is based on Bott (1989a,b) and applies a time step of 20 minutes.

The chemical scheme in the EMEP model includes 140 reactions involving 56 long-lived and 15 short-lived species. The EMEP model couples sulphur and nitrogen chemistry to the photochemistry (Simpson et al., 2003). The model distinguishes between fine (d < 2.5 μm) and coarse (2.5 μm < d < 10 μm) aerosol. The EQuilibrium Simplified Aerosol Model (EQSAM) of Metzger et al. (2002) is used to describe the equilibrium between the different gaseous and inorganic fine aerosol components. EQSAM assumes that the aerosols are internally mixed and that they obey thermodynamical gas/aerosol equilibrium. These assumptions

are sufficiently accurate under most atmospheric conditions considering the 20-minute chemical time step used in the EMEP model. The version used in this thesis calculates a thermodynamic equilibrium of the SO_4^{2-},-NO_3^-, -NH_4^+, -Na^+, -Cl^-, -H_2O system. EQSAM thus accounts for the formation of fine NO_3^- associated with ammonium nitrate (NH_4NO_3) and allows for the formation of NO_3^- on sea-salt aerosol. The input of Na^+ and Cl^- is set to zero, and the EQSAM module is used only for the formation of nitrate associated with ammonium. Coarse nitrate is calculated as the HNO_3 concentration multiplied by a reaction coefficient k_{RH} (in s^{-1}) that depends on the relative humidity, RH:

$$\begin{aligned} k_{RH} &= 1.0 \times 10^{-4} \quad \text{for RH > 90\%} \\ k_{RH} &= 5.0 \times 10^{-6} \quad \text{for RH < 90\%} \end{aligned} \tag{3.1}$$

This calculation is assumed to represent reactions of HNO_3 on both dust and sea-salt.

Dry deposition depends on the aerodynamic resistance between a reference height and the canopy, the quasi-laminar layer resistance to the gas and the surface resistance to the gas. Under normal conditions the surface resistance of HNO_3 is effectively zero, but for numerical reasons it is given a minimum value of 1s m^{-1}. For sub-zero temperatures it follows the formulation of Wesely (1989). This gives HNO_3 its high dry deposition velocity (2 to 5 cm s^{-1}). Dry deposition of aerosols depends on their size. All the resistances are integrated over the aerosol sizes assuming a log-normal size distribution, which is presently assigned the maximum diameters of 0.3 μm and 4 μm and geometric standard deviations of 2.0 and 2.2 μm for fine and coarse aerosols, respectively. The dry deposition velocities of aerosols range from a few millimeters to a few centimeters per second.

Sea-salt is present in two size modes, fine and coarse, as other aerosols in the EMEP model. The formation of sea-salt aerosols larger than 2 μm is parametrized with the empirical expression of Monahan et al. (1986):

$$\frac{dF}{dr_w} = 1.373 U_{10}^{3.41} {r_w}^{-3} (1 + 0.057 {r_w}^{1.05}) \times 10^{1.19 exp(-B^2)} \tag{3.2}$$

in $m^{-2}s^{-1}\mu m^{-1}$ where dF/dr_w is the rate of sea-salt droplets generated per unit area of sea surface per increment of droplet radius dr_w. r_w is the wet radius, U_{10} is the wind speed at 10 m above sea level and B=(0.380-logr_w)/0.650. For sea-salt

smaller than 1μm the parametrization of Mårtensson et al. (2003) is used:

$$\frac{\mathrm{dF}}{\mathrm{dlogD_d}} = 3.84 \times 10^{-6}(\mathrm{A_k T_w} + \mathrm{B_k})\mathrm{U_{10}^{3.41}} \tag{3.3}$$

where dF/dlogD_d is the rate of sea-salt droplets generated per unit area of white cap cover and per increment of droplet dlogD_d. D_p is the dry diameter, A_k and B_k are the empirical coefficients describing the dependence of F on the aerosol size, T_w is the temperature of seawater and U_{10} is the wind speed at 10 m above sea level. The production of sea-salt spray is calculated in seven size bins, which are then aggregated to fine and coarse aerosol fractions.

Both natural dust (desert and soil erosion) and anthropogenic dust are accounted for in the EMEP model. Dust from the Saharan desert beyond the EMEP domain is accounted for through the boundary conditions. Monthly dust concentrations are taken from the global chemical transport model developed and used at the University of Oslo (Grini et al., 2005). The parametrization from erodible soils within the model domain describes both saltation and sandblasting effects. If the friction velocity exceeds a critical friction velocity (u_*>u_{*th}) the mobilisation of particles from the soil surface will occur. The critical friction velocity is calculated using the partitioning scheme of wind shear stress between erodible and non-erodible surface elements (Marticorena and Bergametti, 1995). The horizontal saltation flux of larger soil particles Q_s (kgm^{-1}s^{-1}) is calculated by:

$$\mathrm{Q_s} = \frac{\mathrm{K}\rho_{\mathrm{air}}}{\mathrm{g}}\mathrm{u_*^3}\left(1 - \frac{\mathrm{u_{*th}}}{\mathrm{u_*}}\right)\left(1 + \frac{\mathrm{u_{*th}}}{\mathrm{u_*}}\right)^2 \tag{3.4}$$

where K is the parameter describing soil erodibility, i.e. the accessibility of erosive soil elements. Sandblasting releases smaller particles in the size fraction j in a vertical flux E_j (kgm^{-2}s^{-1}) and is calculated as:

$$\mathrm{E_j} = A_s \alpha \beta_j \mathrm{Q_s} \tag{3.5}$$

where A_s is the area fraction of erodible soil, α is the sandblasting efficiency (m^{-1}), and β_j is the fraction of dust flux in the size fraction j (Tsyro, 2008, and references therein).

3.2 Experimental setup

The implementation of nitrate formation on sea-salt and dust in a numerical model is not straightforward and necessitates a number of different model experiments

as well as careful testing. The model simulations run for this thesis include the main experiments reflecting the stepwise implementation of nitrate formation, and the different sensitivity studies performed for each step of the implementation. In Table 3.1 all model experiments and their main features are listed together with the acronyms to be used hereafter. First the EMEP model is run with the original setup (E_std). Secondly, the formation of coarse nitrate on dust is implemented (E_d). Thereafter the formation of coarse nitrate on sea-salt is implemented (E_ss), before both formations are accounted for simultaneously (E_d_ss). This stepwise approach is chosen to see how the two parametrizations affect coarse nitrate production in the EMEP model individually. For both parametrizations additional sensitivity tests are performed, as will be explained in more detail below. Finally fine nitrate formation on dust and sea-salt is accounted for together with the formation of coarse nitrate on dust and sea-salt (E_fine).

E_std	**Standard run with the original EMEP model**
E_d	**Coarse nitrate formation on dust**
E_d_min	Sensitivity test with γ=2.5e-3 and 2% Ca^{2+} content in dust
E_d_max	Sensitivity test with γ=0.2 and 12% Ca^{2+} content in dust
E_d_ca60	Sensitivity test with 62.5% Ca^{2+} content in dust
E_ss	**Coarse nitrate formation on sea-salt**
E_ss_j	Test of Jaenicke (1988) size distribution for sea-salt
E_ss_split	Test with coarse sea-salt separated into 5 size bins
E_d_ss	**Coarse nitrate formation on dust and sea-salt**
E_fine	**Coarse nitrate formation on dust and sea-salt;**
	fine nitrate formation on dust, sea-salt and ammonia

Table 3.1: *List of the different model experiments done in this thesis. The main model experiments following each step of implementation are listed in bold font, while regular font is used for the sensitivity tests.*

Different approaches

The same method is used for reactions on both dust and sea-salt, based on the approach in Hodzic et al. (2006). Reactions 2.17 and 2.16 are treated through a heterogeneous pathway (Goodman et al., 2000; Hanisch and Crowley, 2001) with a kinetic approach assuming a total reaction in the forward direction.

The uptake coefficients for HNO_3 on dust and sea-salt have been measured in laboratory studies and in field campaigns and the values vary among the different publications (Saul et al., 2006; Tolocka et al., 2004; Guimbard et al., 2002; Stemmler et al., 2008; Fenter et al., 1995; Hanisch and Crowley, 2001; Goodman et al., 2000; Liu et al., 2008; Umann et al., 2005). Theoretically the heterogeneous pathway can be described in four steps. The first step corresponds to gas phase diffusion of nitric acid towards the particle surface. The second step accounts for the nitric acid molecule being transferred to the particle surface. This transfer depends on α, the accommodation coefficient, which is a measure of the probability of the nitric acid being absorbed to the surface during a collision. Thirdly the reaction occurs in bulk phase with rate coefficient k. Finally the gaseous product, such as CO_2 or HCl, desorb. The uptake coefficient γ considered hereafter accounts for steps 2 and 3 combined. The different uptake coefficients chosen for HNO_3 reactions with calcite, dolomite an sea-salt will be discussed in the following sections.

An alternative approach is to assume an equilibrium between HNO_3 and dust or sea-salt. Myhre et al. (2006) used this approach to model nitrate and ammonium aerosols in the presence of sea-salt. First the chemistry module calculates the concentration of HNO_3 due to photochemical reactions. The equilibrium model EQSAM then calculates the equilibrium between NH_3 and HNO_3 through reaction 2.14 and the final concentration of HNO_3 after reactions 2.16 and 2.17 (occurring on sea-salt and dust, respectively) have reached equilibrium. The time step in the EMEP model equals 20 minutes, which is sufficient time for fine nitrate to reach equilibrium. Coarse nitrate, on the other hand, may need hours to reach equilibrium, which is why this approach was not chosen in this thesis.

An additional way of modelling coarse nitrate formation is by a full dynamical mass transfer calculation applied to each aerosol size bin. Capaldo et al. (2000) used a hybrid method with an equilibrium assumption for the fine aerosol mode and a dynamic approach for the coarse aerosol mode. This method was not chosen or studied here because of its high computational requirement.

Reaction coefficient

In the parametrization implemented in this thesis the uptake of HNO_3 on dust and sea-salt is defined by a pseudo first-order reaction coefficient, k:

$$k = \left(\frac{d}{2D_g} + \frac{4}{\nu\gamma} \right)^{-1} A \tag{3.6}$$

where d_l is the particle diameter (m), D_g is the gas phase diffusion coefficient (m^2s^{-1}) (D_g=0.1cm^2s^{-1} from Dentener (1993)), ν is the mean molecular velocity, A is the aerosol surface area, and γ is the uptake coefficient of reactive species. The first part ($d/2D_g$) describes the gas-phase diffusion to the aerosol, while the second part ($4/\nu\gamma$) is the collision rate term describing the uptake of the gas on the surface.

Aerosol surface

The aerosol surface used in the pseudo first-order reaction coefficient k, is the surface of the reactive part in the dust and sea-salt aerosol. The aerosol surface is calculated by using the dimensionless volume fraction (V_f) of the reactive part in dust and sea-salt:

$$V_f = \frac{SM}{A_0\rho} \tag{3.7}$$

where S is the concentration of the reactive part (calcite, dolomite or sodium chloride), M is the molecular weight of the reactive part, A_0 is Avogadro's number and ρ is the density of the aerosol (2.6 g/cm^3 for dust and 2.2 g/cm^3 for sea-salt). With this volume fraction the reactive aerosol surface can be calculated. The ratio between total surface and total volume must be known for each aerosol type (dust and sea-salt). In the EMEP model only fine and coarse aerosols exist. The coarse fraction will be used in the formation of coarse nitrate. The atmospheric aerosol size distribution can be expressed as a trimodal log-normal distribution from Jaenicke (1988):

$$\frac{dN(r)}{d(log(r))} = \sum_{i=1}^{3} \frac{n_i}{\sqrt{2\pi} log\sigma_i} exp \left\{ -\frac{(log\frac{r}{R_i})^2}{2(log\sigma_i)^2} \right\} \tag{3.8}$$

where r is the aerosol radius (in μm), N(r) is the cumulative aerosol number distribution (in cm^{-3}) for aerosols larger than r, R_i is the mean aerosol radius (in μm), n_i is the number concentration and σ_i is the standard deviation of the i^{th} log-normal mode. The trimodal log-normal distribution is a size distribution for the

whole spectrum of aerosols, both fine and coarse, where the three modes represent the nucleation mode, accumulation mode and coarse mode. The surface area of coarse aerosols can then be calculated by solving equation 3.9 by using the third mode:

$$A = V_f \frac{\int_0^\infty 4\pi r^2 \frac{dN(r)}{dr} dr}{\int_0^\infty \frac{4}{3}\pi r^3 \frac{dN(r)}{dr} dr} \tag{3.9}$$

Solving the integral yields:

$$A = V_f \frac{3}{R_i} exp\left\{-\frac{5}{2}(ln\sigma_i)^2\right\} \tag{3.10}$$

This way of calculating the aerosol surface gives a strong dependence on the mean radius and standard deviation given in the trimodal log-normal size distribution. The size distributions of dust and sea-salt depend on the source area and the distance from the sources. For example the size distribution of dust changes as the gravitational settling increases with distance and transport time. The size distribution of dust also depends on the mineralogy of the source area and the extent of particle erosion leading to particle entrainment in the atmosphere. The morphology of dust changes with increasing wind erosion. Erosion processes may change the size distribution of different dust events from the same source region. This dependence on the choice of size distribution represents a rather high uncertainty in this implementation, which is why sensitivity tests are performed for the implementation of coarse nitrate formation on sea-salt.

3.2.1 Coarse nitrate on dust

In this thesis only reactions involving calcite ($CaCO_3$) and dolomite ($CaMg(CO_3)_2$) on dust are considered, as these are the most reactive components of dust (Usher et al., 2003; Krueger et al., 2004; Vlasenko et al., 2006). A heterogeneous pathway of reactions on dust is assumed. In laboratory studies it has been suggested that reactions on dust such as reaction 2.17 are not surface-limited and continue irreversibly until full consumption of reactants has occurred. Kelly and Wexler (2005) showed that reaction 2.17 is a simplified scheme of the more realistic reaction 3.11:

$$2\,\mathrm{HNO_3(g)} + \mathrm{CaCO_3(g)} + \mathrm{nH_2O} \rightleftharpoons \mathrm{Ca(NO_3)_2(nH_2O)(s)} + \mathrm{H_2O} + \mathrm{CO_2(g)} \tag{3.11}$$

where the forward direction is thermodynamically preferred in low-RH conditions, which often occur in the troposphere. Vlasenko et al. (2006) measured an

increase in the uptake coefficient with increasing RH. Nitrate has been recorded in calcium containing anthropogenic dust in Beijing, (Daizhou et al., 2005). The same reactions between HNO_3 and dust components are assumed for both anthropogenic dust and natural dust. The same uptake coefficient of HNO_3 and size distribution of dust are used for anthropogenic dust as for natural dust, as there are no suggestions for the uptake coefficient of HNO_3 found in the literature.

Uptake coefficient of HNO_3

HNO_3 uptake on solid surfaces (γ) has been studied in several laboratory studies with the Knudsen cell technique to measure the reaction rate. In these studies a wide range of values for γ has been found, from 2.5×10^{-4} to 0.2 (Fenter et al., 1995; Hanisch and Crowley, 2001; Goodman et al., 2000). Liu et al. (2008) studied the heterogeneous reaction kinetics of HNO_3 with calcite over a range of RH with a particle-on-substrate stagnation flow reactor, and they found that γ increased with RH, from 0.0032 at RH = 10% to 0.21 at RH = 80%. In the MINATROC (Mineral Dust and tropospheric Chemistry) project Umann et al. (2005) estimated γ from field measurements at the mountain plateau station Izaña in Tenerife, and they found a mean value of $\gamma = 0.033\pm0.017$ based on six different dust events. According to the authors this value represents a lower limit for γ as there might be an underestimation of the effective reaction time of mineral dust-HNO_3. Umann et al. (2005) did not find any dependence on RH in γ, but RH rarely exceeded 40% in the six dust events. The γ from measurements is thus in the same range as the values from the laboratory studies.

In this thesis the uptake coefficient $\gamma = 0.1$ has been used. This is the same value as Hodzic et al. (2006) used for calcite and dolomite, and it is well within the measured γ range from laboratory studies.

Size distribution

In the EMEP model version used in this thesis coarse and fine dust are present, which again are separated in natural dust (dust from the Sahara desert and windblown dust) and anthropogenic dust, as mentioned in section 3.1. The size distribution for dust chosen here is mode 2 of the trimodal log-normal size distribution of background dust from Zender et al. (2003, (their Table 1)) with a mean diameter d = 3.19 μm and standard deviation σ = 1.9. Mode 2 is the mode that dominates long-range transport. The main contributor of natural dust in the EMEP model is

dust from long-range transport from the Saharan desert. The size distribution of dust will, in reality, depend on the type of soil in the source area and on the kind of pollutants the dust-containing air masses have been transported through. The assumption of one single size distribution of dust over the whole EMEP area is thus a simplification.

Chemical composition

There is no chemical speciation of dust in the EMEP model. Therefor a fixed chemical composition of dust had to be assumed in this thesis. This is a very simplified assumption, as the chemical composition of dust is rather complex in reality and depends on its source and on the other pollutants in the transported air masses containing the dust. Loÿe-Pilot et al. (1986) observed calcite contents from Saharan dust in the range 5-30%. This corresponds to 2-12% Ca^{2+} content by mass. For natural dust a content of 5% Ca^{2+} by weight is assumed as proposed in Dentener et al. (1996) and Liao et al. (2003). This value is higher than the value of 4.2% Ca^{2+} content used by Feng and Penner (2007) and the global average of 3.6% suggested in Jaenicke (1988). For anthropogenic dust 4.6% Ca^{2+} content is assumed. This average value of Ca^{2+} over Europe is taken from Loon et al. (2005).

Sensitivity tests

A range of values has been obtained from measurements and laboratory studies for the uptake coefficient of HNO_3 on dust, from 2.5×10^{-3} to 0.2 (Goodman et al. (2000); Fenter et al. (1995), respectively). The Ca^{2+} content in Saharan dust is measured to range from 2-12% (Loÿe-Pilot et al., 1986). To study how sensitive model results of the parametrization of coarse nitrate formation on dust is to these parameters two model runs were performed. First, a model run with the minimum values of the uptake coefficient and Ca^{2+} content in dust, called E_d_min, has been done. A second model run, called E_d_max, has been performed with the maximum values. The dependence on each of the parameters can not be determined separately here as both parameters have been changed simultaneously in each of the first two sensitivity runs. The changes in the reaction coefficient k due to these changes are not linear. The main task of these tests is to give a range of coarse nitrate formation due to the different values proposed for the uptake coefficient of HNO_3 and Ca^{2+} content in dust.

A third model run, E_d_ca60, was devised after the evaluation of the first two sensitivity studies, where a clear negative bias in coarse nitrate was found. In E_d_ca60 the Ca^{2+} content in dust was adjusted to 62.5% to match some of the Ca^{2+} concentrations measured in air at EMEP stations during the intensive campaigns. The aim was to test if the negative bias in coarse nitrate could possibly be connected with the assumption on Ca^{2+} content in dust.

3.2.2 Coarse nitrate on sea-salt

The implementation of the formation of coarse nitrate on sea-salt is equivalent to the implementation of coarse nitrate on dust. The rate-limiting step for reaction 2.16 is suggested to be the formation or release of HCl and not the HNO_3 uptake on the sea-salt surface (Tolocka et al., 2004). When HCl is released in clean air it is stable, but in polluted air it might undergo reaction with $^{\bullet}OH$ and generate reactive $Cl^{\bullet}$. The generation of $Cl^{\bullet}$ atoms in the lower atmosphere can result in either ozon depletion or ozon formation (Pandis and Seinfeld, 1998).

Uptake coefficient of HNO_3

The uptake coefficient of HNO_3 on sea-salt has been investigated in several studies (Stemmler et al., 2008; Liu et al., 2007; Saul et al., 2006; Tolocka et al., 2004; Guimbard et al., 2002)). The range of γ varies from $4.9\times10^{-3}\pm 2.7\times10^{-3}$ (Tolocka et al., 2004) to 0.5 $\pm$ 0.2 (Guimbard et al. 2002; Stemmler et al. 2008). Several factors contribute to the large range of measured γ values. γ depends on RH and the chemical composition and size of the sea-salt aerosol. The nitrate containing salt produced by reaction 2.16 is more hygroscopic than pure NaCl and does not readily crystallize. The presence of nitrate causes NaCl to attain a liquid phase near or at its defects (steps and edges on the droplets surface), and the reaction of the liquid phase of NaCl is known to be faster than the reaction involving the solid phase (Liu et al., 2007). Liu et al. (2007) tested γ for aerosol sizes in the range from d = 1.1 μm to d = 3.4 μm and for RH from 20-80%, and found a peak at d $\sim$0.9 μm and RH = 55% for three different types of salt (pure NaCl, a mixture of NaCl and $MgCl_2$, and real sea-salt particles) with γ being well above 0.2. In this thesis we use γ = 0.2.

Size distribution

Sea-salt in the EMEP model is separated in two size bins, fine and coarse. To calculate the aerosol surface in the coarse sea-salt one needs to know the size distribution of sea-salt. In this thesis a trimodal log-normal size distribution is assumed, where the second mode with number mean dry radius = 1 μm and σ = 2 from O'Dowd et al. (1997) has been used for coarse sea-salt. Mode 2 is the mode for jet droplets, which represent the main source of coarse sea-salt in the EMEP model. Mode 1 is the mode for film droplets, which represent the main source of fine sea-salt in the EMEP model. Mode 3, which is not implemented in the EMEP model, is the mode for spume droplets. As long as RH > 80% sea-salt has a wet radius, while in a dryer environment sea-salt will dry out and have a dry radius. The wet radius for a droplet with dry radius of 1 μm is 2 μm. In this thesis the wet radius of mode 2 is used.

Sensitivity tests

The choice of size distribution from O'Dowd et al. (1997) is arguable. The values from that article are from measurements done in the North-Eastern Atlantic Ocean, and values in the Mediterranean Sea may be different. The aerosol surface calculation depends strongly on the number mean radius and the standard deviation. A model run with a different trimodal log-normal size distribution is done to see how much this affects coarse nitrate formation on sea-salt. In this model run, E_ss_j, mode number 3 with number mean radius of 0.29 μm and σ = 2.5 is used in the trimodal log-normal size distribution suggested by (Jaenicke, 1988) for marine aerosols. This is the mode for large or accumulation particles. Mode 3 from the size distribution of Jaenicke (1988) has a smaller radius than coarse sea-salt in the EMEP model, which is in the range from 2.5 μm to 10 μm.

The size distribution from Jaenicke (1988) is not a realistic choice because of its low number mean radius. Therefor a second model run, called E_ss_split, is done where coarse sea-salt is divided into five different size bins, rather than the three different size bins in the usual model setup. While in the other model runs three sea-salt bins are aggregated to coarse sea-salt, here all the five different bins are kept to get a smoother size distribution. The different size bins and corresponding mean dry and wet radii are listed in Table 3.2, together with the dry deposition velocities used in each bin. The dry deposition velocities are taken from Pryor et al. (2008, their figure 1). As for E_ss the largest part of sea-salt exists in areas with

Bin number	Bin range in μm	r(dry) in μm	r(wet) in μm	v_d in cms^{-1}
1	0.5 - 0.9	0.71	1.4	0.7
2	0.9 - 1.2	1.06	2.1	1.5
3	1.2 - 1.9	1.41	2.8	2.0
4	1.9 - 2.8	2.29	4.5	2.8
5	2.8 - 5.0	3.16	6.3	3.0

Table 3.2: *The different sizes, mean dry and wet radii, and dry depositions (v_d) for the 5 different bins coarse sea-salt has been divided into. The bin ranges are based on the dry radius.*

RH >80%, and the dry deposition velocity for each size bin is chosen based on the wet radius. The wet radius is also used in the calculation of the aerosol surface. The aerosol surface is calculated with the same method as described in section 3.2, but here one has five different size bins instead of the trimodal log-normal size distribution of sea-salt. The aerosol surface in each bin (assuming internally mixed aerosols in each bin) will be:

$$A_i = V_f \frac{4\pi r_i^2}{\frac{4}{3}\pi r_i^3} = V_f \frac{3}{r_i} \tag{3.12}$$

where V_f is volume fraction as in equation 3.7 and r_i is the radius in each bin. The sticking coefficient is assumed to be equal for all sizes (γ=0.2, as in E_ss).

3.2.3 Fine nitrate on sea-salt and dust

Particulate nitrate can form on fine sea-salt and dust as it does on coarse sea-salt and dust. Fine nitrate can be treated as being in equilibrium as the reactions forming fine nitrate are fast enough to reach equilibrium within the 20-minute time step of the EMEP model. The EQSAM model is used for calculation of these equilibrium reactions. EQSAM is dealing with cations and anions, and a chemical fixed composition is assumed for both sea-salt and dust. Sea-salt is separated into Na^+ and Cl^-. The values for Na^+ and Cl^- used are 31% and 55% by mass, respectively, as in Loon et al. (2005). Dust is separated into calcium (Ca^{2+}), magnesium (Mg^+) and potassium (K^+). For natural dust 5% Ca^{2+} and Mg^+ are used as for coarse dust, and 2% K^+ from Krueger et al. (2004, 2005). For anthropogenic dust 8.81% Ca^{2+}, 1.05% Mg^+ and 1.91% K^+ from Loon et al. (2005) are used.

EQSAM calculates the new equilibrium system between SO_4^{2-}, -NO_3^-, -NH_4^+, -Na^+, -Cl^-, -Ca^{2+}, -Mg^+, K^+, -H_2O, and -HCl. This model run is called E_fine and contains the formation of coarse nitrate on sea-salt and dust, with the same values as used in E_ss and E_d together with formation of fine nitrate on sea-salt and dust and formation of ammonium nitrate.

HCl has been added to the EMEP model in this run. The production of HCl is from the coarse nitrate formation on coarse and fine sea-salt. The same deposition velocities as used in the EMEP model for HNO_3 have been used for HCl. Both HNO_3 and HCl are thought to be perfectly absorbed by plant canopies due to their reactivity and high water-solubility. Their canopy resistance $R_c = 0$. This hypothesis has been supported by several measurements (Huebert and Robert, 1985; Dollard et al., 1987; Meyers et al., 1989; Muller et al., 1993).

3.3 Measurement data

Measurements of aerosols have traditionally been sampled by filtration methods and afterwards been analysed for the chemical composition. This is a straightforward method, but the volatility of ammonium nitrate and reactivity to nitric acid makes this method sensitive to artefacts. Ammonium nitrate can evaporate from the filter, which may lead to underestimation of ammonium nitrate in the measurement. Nitric acid may adsorb to other aerosols at the filters leading to underestimation of HNO_3. A method to stabilise the semi-volatile nitrate is to impregnate the filters with a reagent or to use a reactive type of filter. In the standard EMEP network filter methods are used to measure aerosols. The standard EMEP network does not separate different sizes of aerosols. The Task Force on Measurement and Modelling (TFMM) recommended to conduct coordinated intensive measurements between the EMEP super sites to measure the gas-to-particle distribution. The first sampling periods were set to June 2006 and January 2007.

The measurement data used in this thesis are from the EMEP intensive measurement campaigns in June 2006 and January 2007, together with measurements from the standard EMEP network. The stations that took part in these campaigns and their measured components are listed in Table 3.3. Hereafter the stations will be referred to with their station ID (Table 3.3). The locations of the campaign stations are visualized in Figure 3.2.

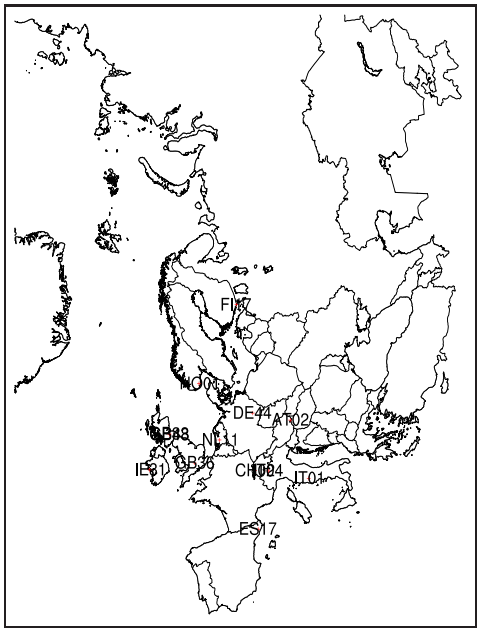

Figure 3.2: *Measurement stations from the campaigns in June 2006 and January 2007*

The hourly PM_1 data are measured by Aerodyne Mass Spectrometers (AMS). This instrument does not determine the size fraction from cut-off of the intake. It measures non-refractory aerosols that vaporize at 550 $\circ$ C, which essentially translates into NH_4NO_3. The hourly data for size fractions other than PM_1 use on-line ion detectors in combination with wet denuders. Systematical biases in the gas/aerosol partitioning in the hourly data (Fagerli and Aas (2008)) are highly unlikely.

Only IT01 has data from daily measurements that are artefact-free. Measurements of PM_{10} and aerosol are using a filter and denuder method and are artefact-free. Other measurement sites apply either low/high volume samplers or filter-packs in the daily measurements.

The model distinguishes only between $PM_{2.5}$ and coarse nitrate. Both PM_1 and $PM_{2.5}$ in the measurements have been compared to $PM_{2.5}$ in the EMEP model. In the hourly measurements that use AMS this is the same as fine nitrate in the EMEP model. Coarse nitrate in the EMEP model is compared to measured nitrate

Station name (ID)	PM_1	$PM_{2.5}$	PM_{coarse}	PM_{10}	aerosol	HNO_3	NH_3
Bush (GB33)	06						
Harwell (GB36)		06	06	06		06	06
Auchencorth Moss (GB48)		06,07		06,07		06,07	06,07
Payerne (CH02)	06						06,07
	06,07			**06,07**			
Melpitz (DE44)	07						
	06,07	**06,07**		**06,07**			
Ispra (IT04)		**06,07**		06,07		06,07	06,07
Cabauw (NL11)		06,07		06,07		06,07	06,07
Montseny (ES17)		**06**[a]		**06**[a]			
Virolhti II (FI17)	**06,07**	**06,07**		**06,07**			
Montelibretti (IT01)		**06,07**	**07**	**06,07**	**07**	**07**	**07**
Birkenes (NO01)	**06**	**06,07**		**06,07**	**07**		
Illmitz (AT02)					**06,07**	**06,07**	**06,07**
Mace Head (IE31)	06						

Table 3.3: *EMEP stations used in the intensive measurement period in June 2006 and January 2007. PM and aerosol are measurements of particle nitrate.*
[a] from the standard EMEP network.
'06': the station measured this component in June 2006.
'07': the station measured this component in January 2007, daily measurement in bold letters, otherwise hourly measurement.

PM_{coarse} or to the difference between measured nitrate PM_{10} and PM_1 or $PM_{2.5}$. At GB48 the measurement of nitrate $PM_{2.5}$ is higher than for nitrate PM_{10} both in June 2006 and in January 2007. Therefor measurements for nitrate PM_{10} and $PM_{2.5}$ from GB48 are not used, neither for 2006 nor 2007. At CH02 nitrate PM_1 exceeds nitrate PM_{10} in the daily measurement. This can be caused by evaporation of NH_4NO_3 on the filter. At this station there were only a few time steps where nitrate PM_1 exceeds nitrate PM_{10} and these were discarded in the evaluation. At NL11 the differences between measurements of nitrate PM_{10} and PM_1 are used when comparing measurements to modelled values. PM_1 is used instead of $PM_{2.5}$ because there are few observations of $PM_{2.5}$.

In the evaluation of the seasonal performance and the gas-to-particle distribution of nitrogen compounds in the EMEP model, measurements from the standard EMEP network are used. In these measurements of particulate nitrate, filter

packs are mainly used with no clearly defined cut-off, but generally around PM_{10}. NH_4NO_3 evaporated from the aerosol front filter can be absorbed by the impregnated filter causing enhanced HNO_3 and NH_3 values (Fagerli and Aas (2008)).

Chapter 4

Results and evaluation

This chapter contains an evaluation of the standard EMEP model followed by evaluations of the different parametrizations implemented in this thesis. Measurements from the EMEP intensive campaigns in June 2006 and January 2007 together with measurements from the standard EMEP network will be used to judge how well the EMEP model performs during summer and winter.

The performance of E_std will be evaluated with respect to nitrogen compounds, sea-salt and dust. The gas/aerosol distribution of ammonia/ammonium and nitric acid/nitrate aerosol will be discussed. The dependence between the different nitrogen compounds, described in chapter 2, makes it important to test how the model manages to reproduce the gas/aerosol distribution. Formation of aerosol nitrate depends among other things on 1) the production of HNO_3, 2) the availability of NH_3/NH_4^+, 3) the temperature, 4) the relative humidity and 5) the deposition velocities of the nitrogen compounds. The distribution of fine and coarse nitrate and the correlation of coarse nitrate are evaluated. The correlation between observations and modelled values of coarse nitrate gives an understanding of how well the EMEP model reproduces the physics of the chemical reactions. The correlation of coarse nitrate in the new parametrization depends on the correlations of both dust and sea-salt, and also on the amount of dust and sea-salt. Therefor, the sea-salt and dust performance of the EMEP model is evaluated in the final section of the evaluation of E_std.

The evaluation of the implementations will focus on how the new model performs compared to the standard model run in terms of nitrogen compounds. Both fine and coarse nitrate in the new implementation are evaluated, and the results are

compared to the results from E_std. The daily correlation is of particular interest in this context, since this is where an improvement can be expected when the dependence of coarse nitrate on dust and sea-salt is taken in account. Finally the gas-to-particle distribution in the new parametrization will be evaluated together with the spatial correlation of coarse nitrate. The spatial correlation is a measure of how well the model reproduces the spatial distribution of coarse nitrate.

Temporal correlation, spatial correlation and bias are used in the evaluations of the model runs. The temporal correlation (hereafter referred to as 'correlation') between measurements y_i and modelled values x_i of a species is calculated as

$$r_{xy} = \frac{\sum_{i=1}^{n}(x_i - \bar{x})(y_i - \bar{y})}{(n-1)s_x s_y} \tag{4.1}$$

where $\bar{x}$ and $\bar{y}$ are the means of x and y , s_x and s_y are the standard deviations of x_i and y_i, and n is the number of measurements. In the calculation of correlations, daily measurements are used unless stated otherwise.

The spatial correlations are calculated in the same way as the temporal correlations, but here x_i and y_i are the means of measurement and modelled values at station i, n is the number of stations and $\bar{x}$ and $\bar{y}$ are the means of x and y over the stations.

The bias is the difference between the arithmetic means of the model and measurements in the period used. Here the percent difference is used as a measure of the bias:

$$\text{Bias} = \frac{100}{n}\frac{\sum_{i=1}^{n} x_i - y_i}{\sum_{i=1}^{n} y_i} \tag{4.2}$$

4.1 Evaluation of the standard Unified EMEP model

This section presents the evaluation of the standard EMEP model run (E_std), which was necessary in order to provide a benchmark against which later improvements related to the new parametrization can be judged.

4.1.1 Gas-to-particle distribution

In this section measurements from the entire standard EMEP network are used. This is done in order to get a broader picture of the gas/aerosol distribution as

there are only few stations in the intensive measurement campaigns. Measurements of total particulate nitrate in June 2006 and in January 2007 are compared to the sum of coarse and fine nitrate in the EMEP model. When comparing model results with measurements it should, however, be kept in mind that the average height of the lowermost sigma layer in the EMEP model amounts to 90 meters. The task of deriving the vertical gradient within this layer is not a straightforward one, which will add to the uncertainty in the comparisons against ground measurements.

NH_3 is underestimated by E_std both in June and January at three Norwegian stations (NO01, NO39, NO15), see Figures 4.1 and 4.2. However, two of the Norwegian stations NO15 and NO39 are known to be situated in environments which experience a strong influence from local ammonia sources (pers. comm. Wenche Aas). This results in a poor spatial correlation in June (Table 4.1). Local sources close to the station give higher values in measurements than the average grid value. Apart from that, the modelled NH_3 agrees with the observations within a factor of 2 at most sites.

There are no systematic differences between the modelled and observed NH_4^+ neither in June nor in January. The stations are evenly spread around the 1:1 line. However the measurements here are from filter packs with a possible negative bias of NH_4^+ (section 3.3).

Nitric acid is underestimated by E_std at some stations and overestimated at others. There seems to be a geographical pattern, e.g. with all Slovakian sites being overestimated and all German sites being underestimated. In general HNO_3 is difficult to model, as is has a short lifetime in the lower troposphere and is involved in a complex equilibrium with NH_3, emissions of NO_x and photochemistry. In these measurements filter packs are used, which are subject to biases. The adsorption of HNO_3 on filters depends on the choice of filter, and the evaporation of ammonium nitrate increases with temperature causing enhanced HNO_3 values (Schaap et al., 2004).

Modelled particulate nitrate is lower than measurements at almost all stations in June. This can be caused by several factors, for example insufficient production of particulate nitrate in the model, too high evaporation of ammonium nitrate during daytime, or too high dry deposition of the aerosols. In January almost all stations are within a factor 2 when comparing model and measurements.

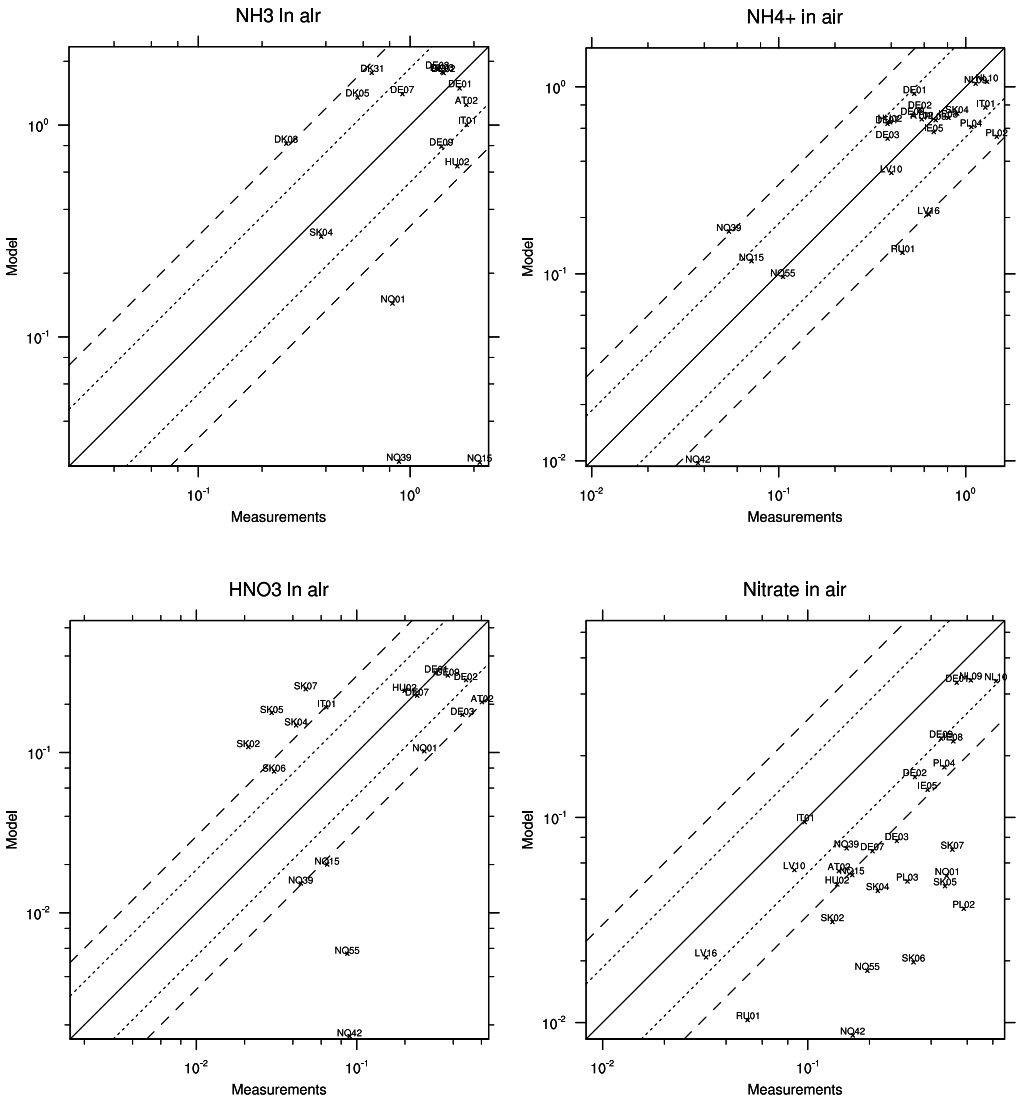

Figure 4.1: *Comparison of modelled NH_3, NH_4^+, HNO_3 and particulate nitrate in E_std and measurements from the standard EMEP network in June 2006. For numbers of the average measurements, modelled average over the stations and correlation see Table 4.1.*

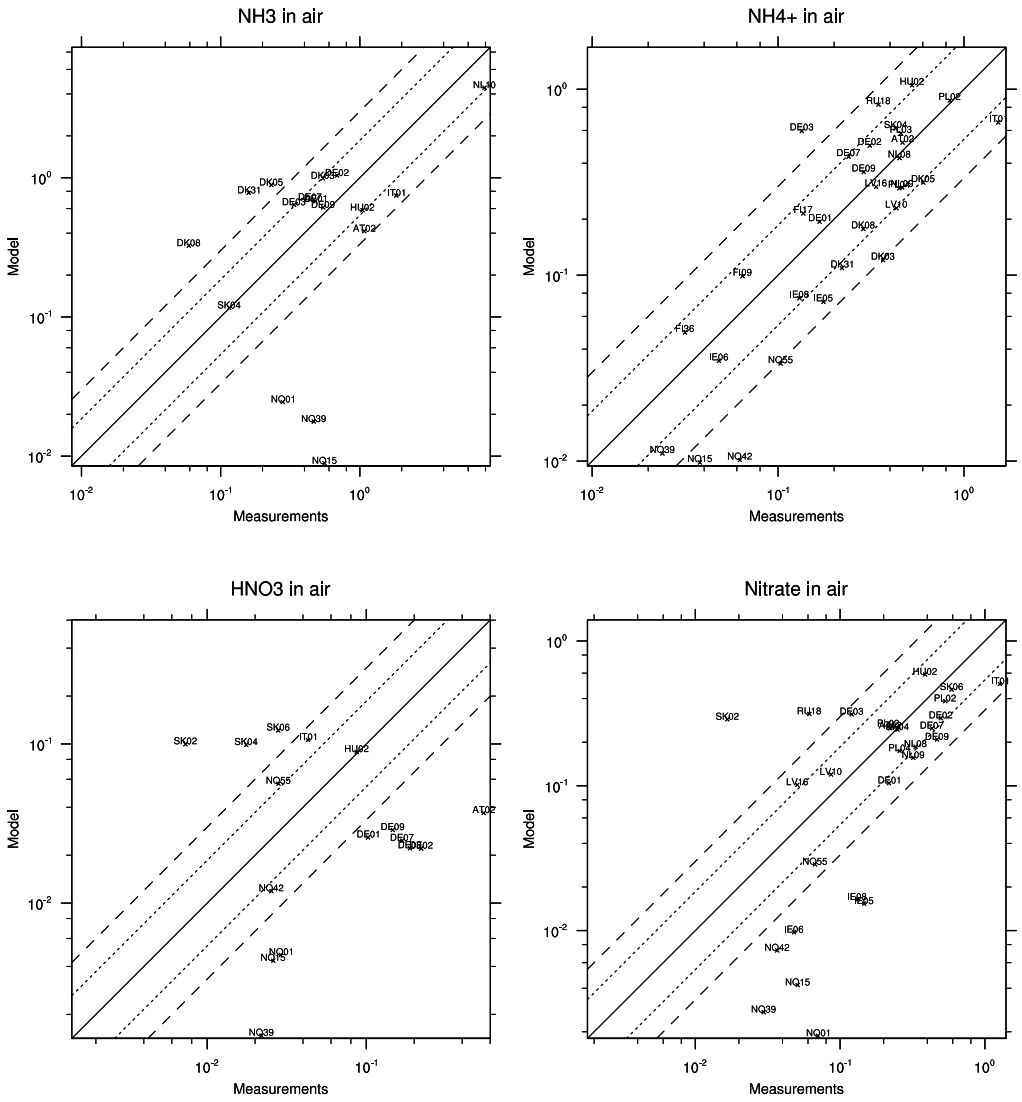

Figure 4.2: *Comparison of modelled NH_3, NH_4^+, HNO_3 and particulate nitrate in E_std and measurements from the standard EMEP network in January 2007. For numbers of the average measurements over the stations, bias and correlation see Table 4.1.*

			E_std		E_d_ss		E_fine	
Component	Obs	Ns	Bias (%)	Corr	Bias (%)	Corr	Bias (%)	Corr
June 2006								
NH_3 in air	1.21	16	-15	0.07	-17	0.07	-15	0.06
NH_4^+ in air	0.62	23	-13	0.68	-7	0.68	-14	0.69
HNO_3 in air	0.19	18	-18	0.54	7	0.52	7	0.52
Nitrate in air	0.32	28	-63	0.71	-75	0.70	-74	0.70
January 2007								
NH_3 in air	0.98	17	-22	0.93	-25	0.93	-22	0.93
NH_4^+ in air	0.33	31	-1	0.62	16	0.64	-3	0.60
HNO_3 in air	0.11	16	-55	-0.22	-23	-0.29	-27	-0.29
Nitrate in air	0.26	27	-23	0.68	-12	0.66	-3	0.67

Table 4.1: *Result from E_std, E_d_ss and E_fine in June 2006 and January 2007, from the EMEP monitoring network. Ns is the number of stations where measurements are available. Obs is the measured monthly average over Ns stations given in μg(N) m^{-3}. Corr is the spatial correlation between observations and model for station monthly averages. See the introduction to Chapter 4 for a definition of bias.*

4.1.2 Amount of fine and coarse nitrate aerosols

In this section only the intensive campaign data are used as these are the only measurements separating fine and coarse nitrate.

Fine nitrate is somewhat underestimated by E_std, both in June and January (Table 4.2). At CH02 there are two parallel methods to measure NO_3^- PM_1, one is based on hourly data (AMS) and the other one on daily data (gravimetric). These two methods give different results, especially in June. The daily data are much lower than the corresponding AMS measurements. This is probably due to evaporation of NH_4NO_3 on the filter in the daily data. The hourly measurements are probably more correct due to artefact-free measurements by using the AMS method (section 3.3). The only other stations with positive biases are IT01 (+84%) and ES17 (+9%) in January.

Coarse nitrate is somewhat underestimated at most stations by E_std both in June and in January, see Figure 4.3 and Table 4.3. At NL11 the EMEP model produces more coarse nitrate than is observed in June (bias of 83% for hourly data). NL11 also measures NH_3, HNO_3 and fine nitrate. NH_3 and fine nitrate are lower in E_std

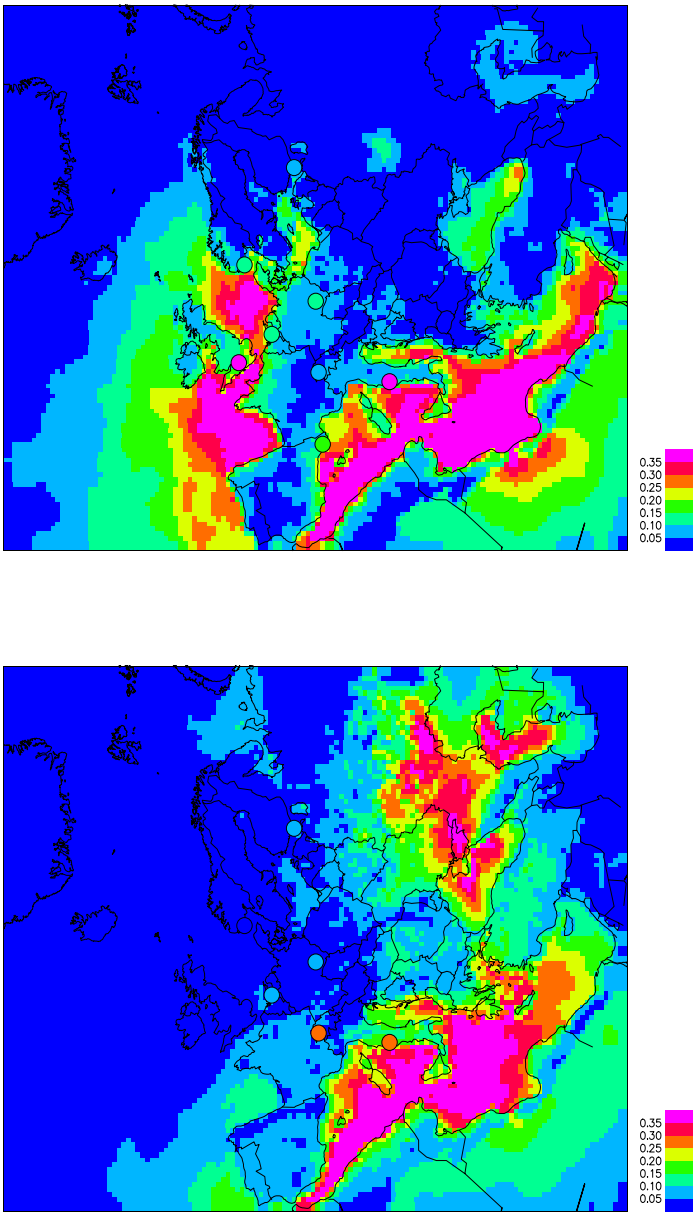

Figure 4.3: *Coarse nitrate in E_std in June 2006, upper panel, and January 2007, lower panel. The bullets are observations of coarse nitrate at the stations from the intensive measurement campaigns. Both measured and modelled coarse nitrate is shown in* $\mu g(N)m^{-3}$.

Station	**Bias (%)**			**Correlation**		
ID	E_std	E_d_ss	E_fine	E_std	E_d_ss	E_fine
			June 2006			
CH02	1000	1100	1100	0.55	0.49	0.49
DE44	-84	-69	-69	0.28	0.37	0.37
FI17	-100	-100	-100	-0.14	-0.26	-0.28
IT01	-100	-98	-98	-0.22	-0.23	-0.23
IT04	-34	-20	-20	0.54	0.53	0.53
NO01	-99	-86	-71	0.17	0.36	0.31
ES17	-33	0	0	0.71	0.66	0.69
CH02	**-50**	**-27**	**-32**	**0.30**	**0.31**	**0.30**
GB33	**-91**	**-82**	**-76**	**0.66**	**0.66**	**0.63**
GB36	**-78**	**-67**	**-63**	**0.45**	**0.44**	**0.43**
IE31	**-89**	**-50**	**400**	**0.13**	**0.20**	**-0.02**
NL11	**-79**	**-72**	**-70**	**0.67**	**0.69**	**0.69**
			January 2007			
CH02	-47	-23	-19	0.69	0.68	0.67
DE44	-32	0	5	0.51	0.62	0.63
FI17	-20	0	40	0.13	0.20	0.34
IT01	84	200	211	0.04	0.17	0.17
NO01	-93	-70	377	-0.10	-0.10	0.23
ES17	9	43	35	-0.91	-0.88	-0.88
CH02	**-70**	**-58**	**-55**	**0.58**	**0.54**	**0.53**
NL11	**-44**	**-24**	**-15**	**0.71**	**0.71**	**0.70**
DE44	**-24**	**2**	**7**	**0.67**	**0.69**	**0.69**

Table 4.2: *Bias and correlation between measurements and model runs E_std, E_d_ss and E_fine for fine nitrate. Bold numbers are based on hourly data, others on daily data. Either PM_1 or $PM_{2.5}$ from measurements are compared to $PM_{2.5}$ in the model depending on availability.*

Station	Bias (%)				Correlation			
ID	E_std	E_ss	E_d	E_d_ss	E_std	E_ss	E_d	E_d_ss
				June 2006				
CH02	-40	-100	-97	-96	-0.26	-0.03	0.56	0.53
GB36*	-59	-96	-100	-94	0.05	0.39	-0.18	0.39
NL11*	133	-63	-98	-61	0.18	-0.15	0.32	-0.12
FI17	-3	-92	-99	-92	0.44	0.66	0.00	0.66
IT01	-64	-97	-94	-91	0.17	-0.06	0.36	0.22
NO01	-35	-91	-100	-91	0.49	0.62	0.13	0.62
DE44	5	-96	-99	-96	0.11	0.56	-0.13	0.54
ES17	-30	-95	-85	-79	0.14	-0.46	0.84	0.75
				January 2007				
CH02	-79	-97	-100	-98	0.39	0.52	0.30	0.53
NL11*	-64	-89	-100	-89	0.11	0.06	0.13	0.06
FI17	-27	-96	-100	-95	-0.03	0.05	0.07	0.05
IT01	-30	-87	-99	-85	0.06	0.22	0.00	0.21
NO01	16	-74	-95	-74	0.06	0.33	0.14	0.33
DE44	-50	-90	-100	-95	0.24	0.39	0.15	0.39

Table 4.3: *Bias and correlation between measurements and model runs E_std, E_d, E_ss and E_d_ss for coarse nitrate. At the stations marked with an asterisk have hourly measurements, here the daily averages are used to calculate the correlations.*

than what is observed, while HNO_3 have higher values in E_std in June. Low values of NH_3 cause less fine nitrate and hence excess HNO_3 to form coarse nitrate. Lower modelled NH_3 values can be caused by, for instance, 1) an overestimation of dry deposition, 2) local sources, and 3) chemistry.

In general E_std tends to produce low values of fine (and to some extent coarse) nitrate, compared to observations.

4.1.3 Day-to-day correlation of coarse nitrate

The measurements from the intensive campaigns in June 2006 and January 2007 are used here. The correlations are relatively low in both summer and winter. The

highest correlation is 0.49 at NO01 in June (see Table 4.3 for correlation at the other stations in June and January). In general, the model does not reproduce the peaks of coarse nitrate. This is probably due to higher coarse nitrate formation during dust events and days with high sea-salt emissions in reality, while in E_std coarse nitrate formation depends only on HNO_3 and RH.

4.1.4 Ca^{2+} in dust

To evaluate the Ca^{2+} content in dust, measurements of Ca^{2+} are compared to the sum of 5% of the natural dust, 4.6% of coarse anthropogenic dust, and 8.8% of fine anthropogenic dust in the EMEP model (Figure 4.4), as the parametrization of coarse nitrate formation on dust assumes a fixed chemical composition (section 3.2.1). This is a considerably simplified assumption since the chemical compos-

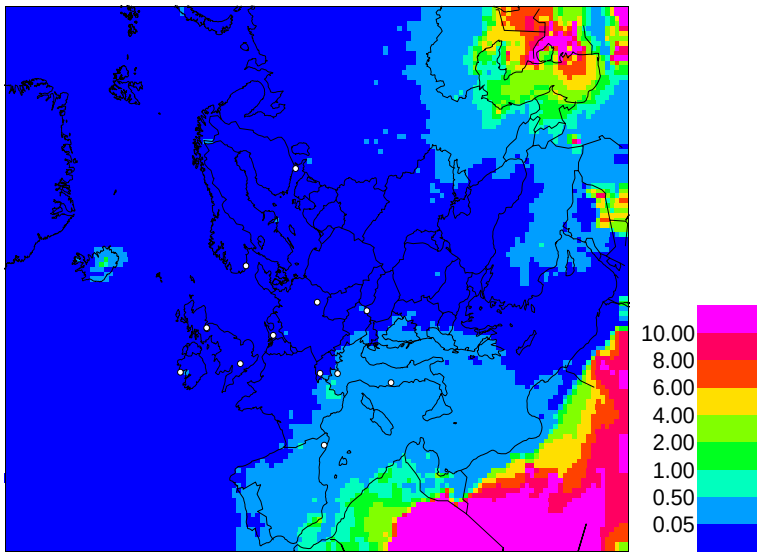

Figure 4.4: *Monthly mean of assumed Ca^{2+} content in dust in the EMEP model in June 2006 in $\mu g\ m^{-3}$, see text for details. The white dots mark the location of the 13 stations from the intensive measurement campaigns.*

ition of dust changes from region to region as discussed in section 3.2.1. With this assumption on the Ca^{2+} content in dust, Ca^{2+} is considerably underestimated by E_std, as can be seen from comparisons at 24 stations in the standard EMEP

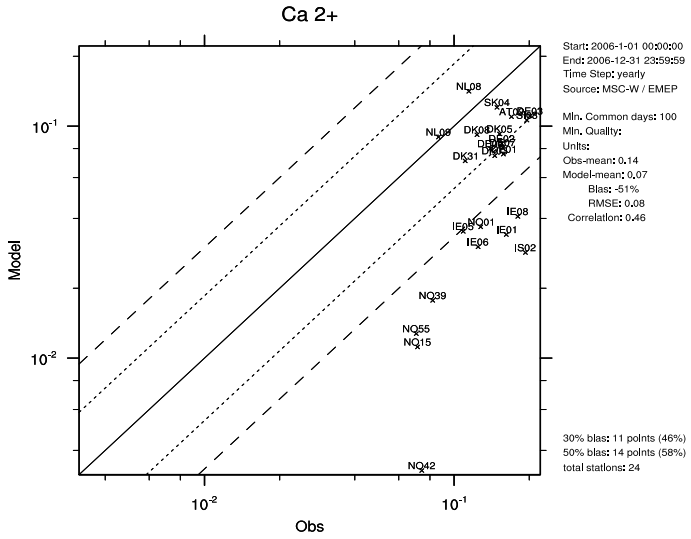

Figure 4.5: *Scatterplot of the model performance on dust compared with measurement of Ca^{2+}. The total PM amount of Ca^{2+} in 2006 from the standard EMEP network is compared to 5% of natural dust, 4.6% of coarse anthropogenic dust and 8.8% of fine anthropogenic dust in the EMEP model.*

network during the whole year of 2006 (see Figure 4.5). The bias and spatial correlation over the 24 stations are -51% and 0.46 respectively. In the year 2006 these 24 stations have highest underestimation from April to August, a negative bias is also seen in autumn. In June 2006 and January 2007 there is a negative bias of -73% in both months at the 24 stations (not shown). The lower values of Ca^{2+} in the model compared to measurements can be caused by several factors, for example the assumed Ca^{2+} content in natural and/or anthropogenic dust might be too small. Anthropogenic dust emissions are also very uncertain. Few measurements exist of total dust. In the intensive measurement periods there are two stations that measure all the components in mineral dust. Evaluation of PM_{10} of dust at ES17 and IT01 reveals an overestimation at ES17 in both months and an overestimation in June at IT01 and underestimation in January (Tsyro and Aas, 2008). In general, total dust seems to be reproduced relatively well. For more data of dust in the EMEP model see Tsyro and Aas (2008). As the Ca^{2+} content is underestimated by the EMEP model, the assumption of 5% Ca^{2+} in natural dust is probably too low.

Measurements of Ca^{2+} in both PM_{10} and PM_1 exist for 5 stations (IT01, ES17, DE44, FI17 and NO01) in the intensive measurement periods. The difference between measured PM_{10} and PM_1 is compared to 5% of the coarse natural dust and 4.6% of coarse anthropogenic dust in E_std. This comparison reveals a negative bias both in June and January (-92% and -95%, respectively). At IT01 and ES17 total dust is overestimated in June, the assumption of 5% Ca^{2+} content in natural dust is probably too low, at least at these stations. Negative biases of coarse nitrate are therefor expected at these 5 stations.

4.1.5 Sea-salt

Measurements of Na^+ concentration in air are compared to modelled Na^+ (31% of the sea-salt in E_std) to evaluate sea-salt (Figure 4.6), as a chemical fixed composition of sea-salt is assumed (section 3.2). Measurements from 22 stations in the standard EMEP network are compared with E_std during the whole year of 2006 (see Figure 4.7). This comparison shows that E_std overestimates Na^+ concentrations by 25% on average. The average spatial correlation is 0.78. Seasonal verification of Na^+ gives a bias of 27% in winter, 14% in spring, -13% in summer, and 18% in autumn (pers. comm. Svetlana Tsyro, EMEP status report 4/2009 to be submitted).

In the intensive measurement periods there are measurements of Na^+ in PM_{10} (Na_PM_{10}) and in $PM_{2.5}$ ($Na\_PM_{2.5}$). Modelled coarse Na^+ is compared to the difference between measured Na_PM_{10} and $Na\_PM_{2.5}$. In June there is a negative bias of -75% and a spatial correlation of 0.49 at the 5 stations (FI17, NO01, IT01, DE44 and CH02) with measurements. In January the bias is -52% and the mean correlation is 0.77 at the same 5 stations as in June. A closer examination of the intensive measurements data shows that E_std underestimates both Na_PM_{10} and $Na\_PM_{2.5}$. The differences between measurements from the monitoring network and the intensive measurement periods are probably not due to different artefacts, as daily measurements are used. The differences are more likely due to the usage of a different set of stations in the intensive campaigns. This can explain the different biases in the E_std compared to measurements. NO01 is the only station that measures air concentration of Na^+ in the EMEP monitoring network and Na_PM_{10} and $Na\_PM_{2.5}$. This station has a negative bias of less than 30% for the whole year of 2006 and less than 50% in June and January for both comparisons with the intensive periods and the EMEP standard network.

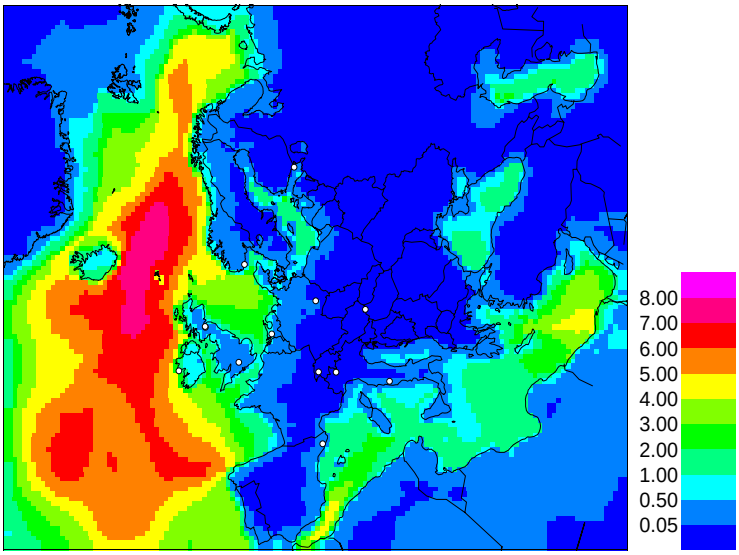

Figure 4.6: *Monthly mean of 31% of coarse sea-salt in the EMEP model in June 2006 in $\mu g\ m^{-3}$, see text for details. The white dots mark the location of the 13 stations from the intensive measurement campaigns.*

In general Na^+ is reproduced well over the whole year compared to measurements of total Na^+, and enough coarse nitrate formation could be expected on sea-salt. However, at the stations used in the intensive measurement periods there is a negative bias of coarse Na^+ and hence a too small formation of coarse nitrate is expected here.

4.2 Coarse nitrate on mineral dust

In this section the parametrization of coarse nitrate formation on dust is evaluated. The results from E_d will be compared to measurements and to E_std. From Figure 4.4 where the assumed Ca^{2+} content in dust in the EMEP model in June is visualized it is clear that improvements can only be expected in the Mediterranean area.

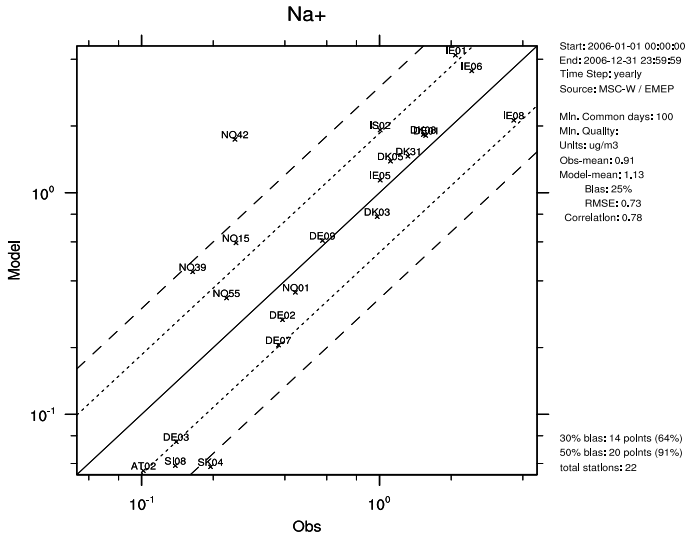

Figure 4.7: *Scatterplot comparing modelled Na^+ with measurements of Na^+. The air concentration of Na^+ from the EMEP monitoring network for 2006 is compared to 31% of total sea-salt in the EMEP model.*

4.2.1 Day-to-day correlation of coarse nitrate

The implementation of coarse nitrate formation on dust improves the correlation at some stations and worsens it at others, see Table 4.3. There is improvement at the stations relatively close to the Mediterranean Sea (ES17, IT01 and CH02) in June, while at stations further north (e.g. NO01, FI17, GB36 and DE44) the correlation worsens. IT01 is one of the stations with improved correlation (from 0.17 to 0.36). At this station there are also measurements of Ca^{2+}. In Figure 4.8 the measurements of Ca^{2+} are shown together with modelled Ca^{2+}, measurements of coarse nitrate and modelled coarse nitrate in E_std and E_d. A correlation between observed Ca^{2+} and coarse nitrate can be seen, with a delay of one day for coarse nitrate. Formation on dust is probably the main source of coarse nitrate at IT01 in June 2006. The correlation of Ca^{2+} and modelled Ca^{2+} is 0.81, but modelled Ca^{2+} is lower than the measurements. The correlation of coarse nitrate at this station is probably affected by the small amount of Ca^{2+} in the first two weeks of June.

The correlation at the stations that get affected by dust improves. At the sta-

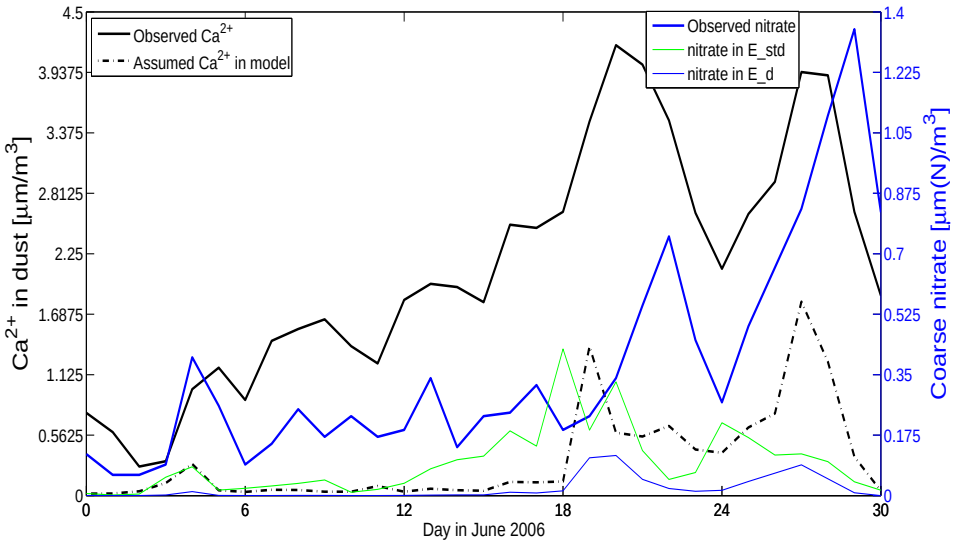

Figure 4.8: *Black lines, left y-axis: Observations of Ca^{2+} at Montelibretti (IT01) and model performance of 5% of natural dust, 4.6% of coarse anthropogenic dust and 8.81% of fine anthropogenic dust (the assumed amount of Ca^{2+} in dust). Colored lines, right y-axis: Observation and model performance of coarse nitrate in June 2006. The correlation between observed Ca^{2+} and observed coarse nitrate is 0.86, the correlation taking into account a time lag of 1 day is 0.89.*

tions without or with small amounts of dust there is either no influence of this implementation or the correlation seems to worsen.

4.2.2 Amount of fine and coarse nitrate aerosol

In E_std, fine nitrate is somewhat underestimated and to some extent also coarse nitrate. In E_d there is less coarse nitrate than in E_std and more fine nitrate. However, there are still, to some extent, smaller values in E_d than in measurements of fine nitrate. The reason for more fine nitrate in E_d is probably that there is less formation of coarse nitrate and therefor more HNO_3 available to react with NH_3 forming fine nitrate. There can be several reasons for the negative bias of coarse nitrate in E_d. At IT01, ES17, DE44, FI17 and NO01 an underestimation of coarse nitrate on dust is expected, as the evaluation of coarse Ca^{2+} content in dust revealed too small modelled values at these stations. The parametrization

depends on the aerosol surface, which is uncertain. The assumption of 5% Ca^{2+} content in natural dust might be too low. There is also a range of different uptake coefficients of HNO_3 on dust from measurements in laboratory studies. Some of these uncertainties have been tested in the sensitivity test runs E_d_min and E_d_max, which are discussed in next section.

4.2.3 Sensitivity tests

To explore the sensitivity of the parameters in the parametrization, two additional runs are performed, as described in section 3.2.1. In these two runs the effects of the uptake coefficient of HNO_3 and the content of Ca^{2+} in dust are tested, by using the lowest and highest values found in the literature for Ca^{2+} content in dust and for the HNO_3 uptake coefficient.

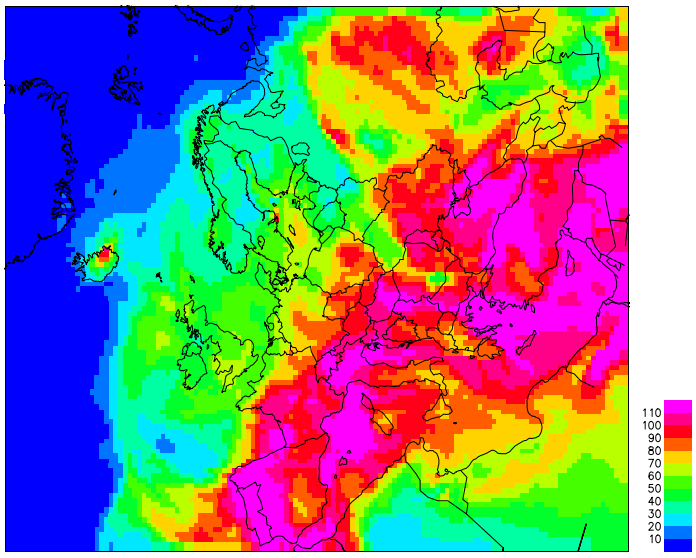

Figure 4.9: *The percent difference of coarse nitrate between E_d and E_d_max in June 2006.*

The change of coarse nitrate from E_d to E_d_max and E_d_min is not linear, which is caused by the non-linearity in the change of the reaction coefficient k. In Figure 4.9 the percent change in coarse nitrate between E_d and E_d_max is shown. As expected, the change in coarse nitrate is highest in the areas over the

Mediterranean, which is the area with most dust and HNO_3.

In Table 4.4 the differences between the sensitivity run and E_d are shown. At IT01, the station near Rome, and at the Spanish coastal station ES17 the effect of the sensitivity test (Figure 4.10) is clearly seen.

June 2006								
Station	**Bias (%)**				**Correlation**			
ID	E_d	E_d_min	E_d_max	E_d_ca60	E_d	E_d_min	E_d_max	E_d_ca60
CH02	-97	-100	-94	-88	0.56	0.07	0.54	0.48
GB36*	-100	-100	-99	-98	-0.18	-0.17	-0.19	-0.05
NL11*	-98	-99	-97	-89	0.32	0.34	0.30	0.31
FI17	-99	-100	-99	-97	-0.30	-0.42	-0.26	0.18
IT01	-94	-100	-89	-81	0.36	0.39	0.37	0.39
NO01	-100	-100	-99	-99	0.13	-0.17	0.11	0.18
DE44	-99	-100	-99	-97	-0.13	-0.19	-0.09	-0.06
ES17	-85	-99	-70	-45	0.84	0.82	0.85	0.86

Table 4.4: *Bias and correlation between measurements and model runs E_d, E_d_min , E_d_max and E_d_ca60 for coarse nitrate in June 2006. The stations marked with an asterisk have hourly measurements, here the daily averages are used to calculate the correlations.*

The differences between monthly means of coarse nitrate in E_d_max and E_d_min in June 2006, are a maximum in the Mediterranean Sea where the difference reaches 0.34 μg(N) m^{-3}. The influence of these sensitivity tests changes over Europe as can be seen from Table 4.4. At IT01 the changes between the E_d_max and E_d_min are 0.039 μg(N) m^{-3}, while the difference at NO01 is 0.001 μg(N) m^{-3}. Measured values at IT01 and NO01 are 0.36 μg(N) m^{-3} and 0.11 μg(N) m^{-3}, respectively.

As the assumed Ca^{2+} content of 5% natural dust revealed a severe underestimation in the EMEP model compared to measurements an additional test of the dust parametrization was done. The results of E_d_ca60 show that there is still a negative bias at the stations where dust plays a significant role. At IT01 coarse nitrate in this model run is of the same magnitude as in the old parametrization during a dust event, where there should be enough Ca^{2+} to give more coarse nitrate (see Figure 4.11). This indicates that at some points it is not only the amount

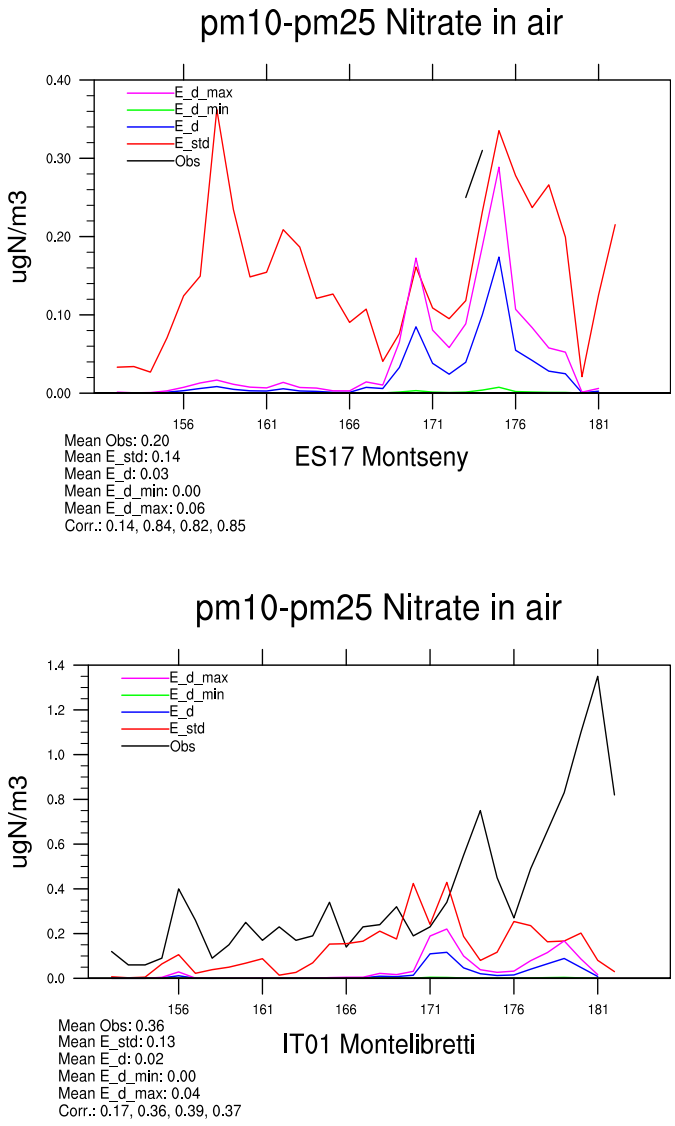

Figure 4.10: *Observed coarse nitrate and modelled coarse nitrate at Montseny (ES17 upper panel) and Montelibretti (IT01 lower panel) in June 2006. Both sensitivity model runs E_d_min and E_d_max are shown together with the standard run E_std and E_d.*

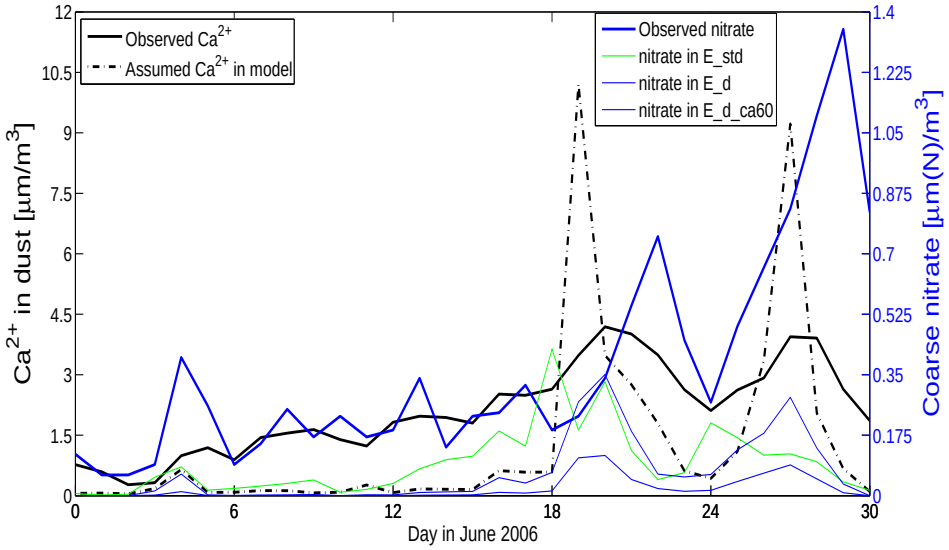

Figure 4.11: *Black lines, left y-axis: Observations of coarse Ca^{2+} at Montelibretti (IT01) and model performance of 62.5% of total coarse dust in the EMEP model. Colored lines, right y-axis: Observation and model performance of coarse nitrate in June 2006.*

of available Ca^{2+}, which affects coarse nitrate formation on dust. In this particular time and place (Figure 4.11) there is probably not enough HNO_3 available as the peak in coarse nitrate in the old parametrization is the same. Over the Mediterranean Sea there is up to 0.55 μg(N) m^{-3} in E_d_ca60. In comparison the value of E_d over the same area is 0.15 μg(N) m^{-3}.

4.2.4 Comparison to other work

Hodzic et al. (2006) implemented coarse nitrate formation on dust in the regional chemistry-transport model CHIMERE. The same method has been used in this thesis as in Hodzic et al. (2006). A fixed chemical composition of dust is assumed both in this thesis and in Hodzic et al. (2006). Hodzic et al. (2006) assumed 17% Ca^{2+} content in dust which is high compared to the assumption of 5% Ca^{2+} content in natural dust and 4.6% in anthropogenic dust as is used in this thesis. More coarse nitrate is expected in their results as their Ca^{2+} content in dust is higher. In Hodzic et al. (2006) there is only formation on natural dust. The total dust in

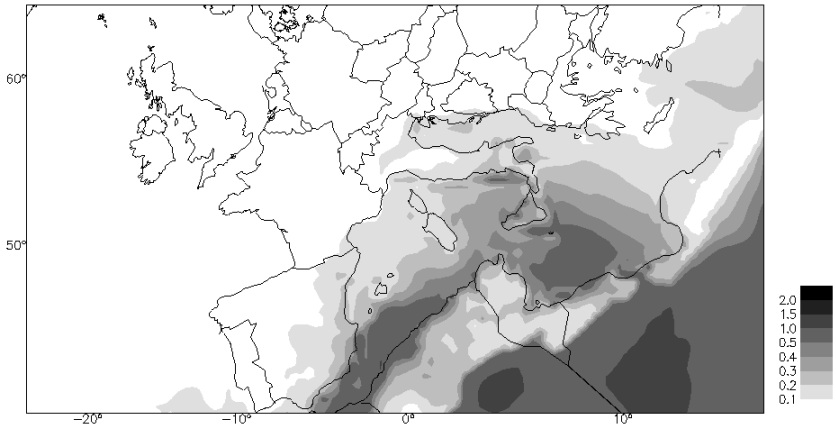

(a) *Average coarse nitrate ($\mu g\ m^{-3}$) in E_d in June 2006 plus January 2007*

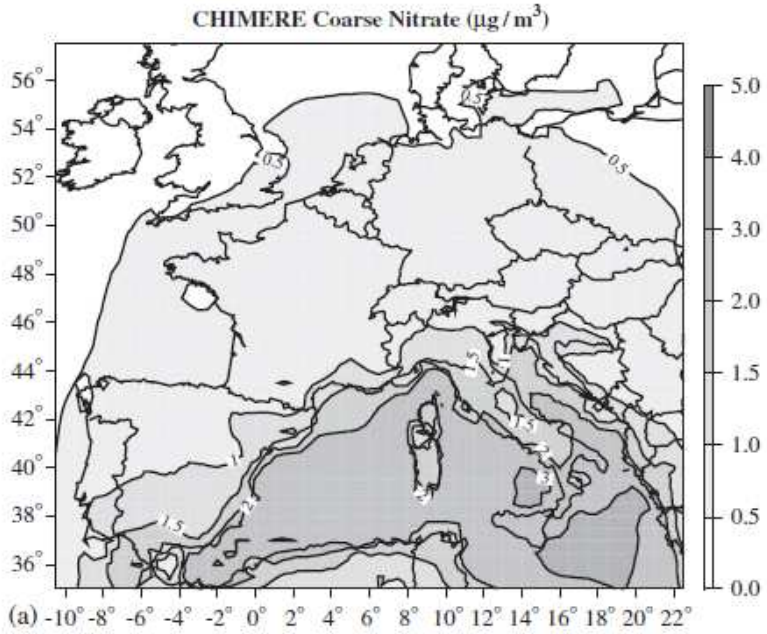

(b) *2001 yearly average of concentration in coarse nitrate ($\mu g\ m^{-3}$) from the study of Hodzic et al. (2006)*

Figure 4.12: *Coarse nitrate from this thesis in a) and figure 4a from Hodzic et al. (2006) in b)*

the EMEP model and natural dust in Hodzic et al. (2006) are in the same range in southern Europe, but in northern Europe there are smaller values of dust in the EMEP model. In Figure 4.12 modelled coarse nitrate from Hodzic et al. (2006) is shown together with modelled coarse nitrate in E_d. In Hodzic et al. (2006) they calculate the annual mean of coarse nitrate, whereas in this thesis monthly means are calculated for June 2006 and January 2007 for E_d. The average of these two months is used for comparison with Hodzic et al. (2006). In E_d there is less coarse nitrate than in the result of Hodzic et al. (2006). The higher Ca^+ content assumed in Hodzic et al. (2006) can explain some of the differences. There are also differences in the calculation of the aerosol surface between this work and Hodzic et al. (2006). In CHIMERE the aerosol distribution is represented by 6 geometrically spaced size bins from 10 nm to 40 μm diameter with internally mixed aerosols in each size bin. In the EMEP model aerosols are represented in two size bins, coarse and fine, and a log-normal size distribution is assumed here to calculate the aerosol surface of the coarse aerosol.

In the sensitivity tests E_d_max has the same values as Hodzic et al. (2006) between Spain and northern Africa, while in all other areas this model run has lower values. E_d_ca60 gives higher values than Hodzic et al. (2006) between Spain and northern Africa, but smaller values elsewhere. The parametrization of coarse nitrate on dust in this thesis does not produce coarse nitrate over large enough areas.

4.3 Coarse nitrate on sea-salt

This section contains an evaluation of the implementation of coarse nitrate formation on sea-salt. The results from this implementation will be compared to the results from E_d and E_std.

4.3.1 Day-to-day correlation

In E_ss an improvement is expected at the coastal stations, and in particular the northern stations, as FI17 and NO01, as these stations are characterized by high amounts of sea-salt (Figure 4.6). The correlation improves at most of the stations in the intensive measurement campaigns compared to E_std both in June 2006 and January 2007. NL11, IT01 and ES17 are not improving in June. At these stations the correlation improved in E_d compared to E_std. Measurements of Na^+

at IT01 are compared to 31% of sea-salt in E_ss and do not correlate well in June, which can explain the lack of improvement in coarse nitrate correlation at this station. Both ES17 and IT01 are stations that are affected by dust, see Figure 4.4. As ES17 is close to the sea an improvement from this implementation of coarse nitrate on sea-salt could be expected. In January 2007 the correlation improves at all stations except NL11.

In the implementation of coarse nitrate formation on sea-salt the daily correlation improves compared to the correlation in E_std. In particular there is an improvement at the northern stations near the coast.

4.3.2 Amount of fine and coarse nitrate

Both coarse and fine nitrate in E_ss are underestimated compared to the intensive measurements in June 2006 and January 2007. The biases range from -100% to -75% for coarse nitrate (see Table 4.3). It should be noted that at FI17, NO01, IT01, DE44 and CH02 there are negative biases of modelled Na^+ compared to measurements. Fine nitrate is underestimated at all stations in June except ES17. In January there are higher values in E_ss than in measurements at some stations and smaller values at others. There is somewhat more fine nitrate in E_ss during winter than in summer. For coarse nitrate there are no clear differences between summer and winter. The formation of coarse nitrate on sea-salt gives more coarse nitrate than the implementation of coarse nitrate on dust. The values of fine nitrate in E_ss and E_d are comparable at the measurement stations both in June 2006 and in January 2007.

The distribution between fine and coarse nitrate reveals an underestimation of both coarse and fine nitrate in E_ss compared to the intensive measurements. The biases for coarse nitrate are higher than for fine nitrate. Coarse nitrate in E_ss is, as expected, mainly formed in the coastal region. There is less coarse nitrate in E_ss than in E_std but more than in E_d. The formation of coarse nitrate on sea-salt is higher than the formation of coarse nitrate on dust.

4.3.3 Sensitivity tests

The choice of one single log-normal size distribution for sea-salt in the implementation of coarse nitrate formation on sea-salt is a simplified assumption. Two sensitivity runs of the EMEP model are done where the size distribution of coarse

sea-salt and hence the formation of coarse nitrate on sea-salt is changed, as discussed in section 3.2.1. The choice of mode 3 of the trimodal log-normal size distribution for marine aerosol from Jaenicke (1988) gives an aerosol surface that is 2.81 times larger than mode 2 from O'Dowd et al. (1997). The reaction rate also depends non-linearly on the radius, see equation 3.6. The choice of a smaller radius will give an even higher reaction coefficient. The second sensitivity test is to separate coarse sea-salt into 5 bins instead of choosing a log-normal size distribution, and to let coarse nitrate form in each bin. In this section the results of these sensitivity tests will be discussed.

June 2006						
Station	**Bias (%)**			**Correlation**		
ID	E_ss	E_ss_j	E_ss_split	E_ss	E_ss_j	E_ss_split
CH02	-99	-97	-99	-0.03	-0.08	-0.07
GB36*	-96	-88	-95	0.39	0.43	0.42
NL11*	-63	5	-56	-0.15	-0.19	-0.18
FI17	-89	-66	-87	0.78	0.81	0.80
IT01	-97	-91	-91	-0.06	-0.10	-0.08
NO01	-91	-78	-90	0.62	0.65	0.62
DE44	-96	-89	-95	0.56	0.65	0.62
ES17	-94	-80	-92	-0.46	-0.50	-0.48

Table 4.5: *Bias and correlation between measurements and model runs E_ss, E_ss_j and E_ss_split for coarse nitrate in June 2006. The stations marked with an asterisk have hourly measurements, here the daily averages are used to calculate the correlations.*

More coarse nitrate is found in E_ss_j than in E_ss which is expected. Also in this simulation a negative bias is seen at all the measurement stations in June 2006 (Table 4.5), and there is less coarse nitrate in E_ss_j than in E_std. The different result of E_ss, E_ss_j and E_ss_split at FI17 and NO01 are shown in Figure 4.13. The monthly mean of coarse nitrate over the whole field in June 2006 is for E_ss_j 0.08 μg(N) m^{-3}, while the monthly mean of coarse nitrate in E_ss is 0.03 μg(N) m^{-3}.

E_ss_split does not give any large differences in coarse nitrate compared to E_ss at the measurement stations. There is a tendence of more coarse nitrate at the measurement stations in E_ss_split. This can be seen in Figure 4.14 where the

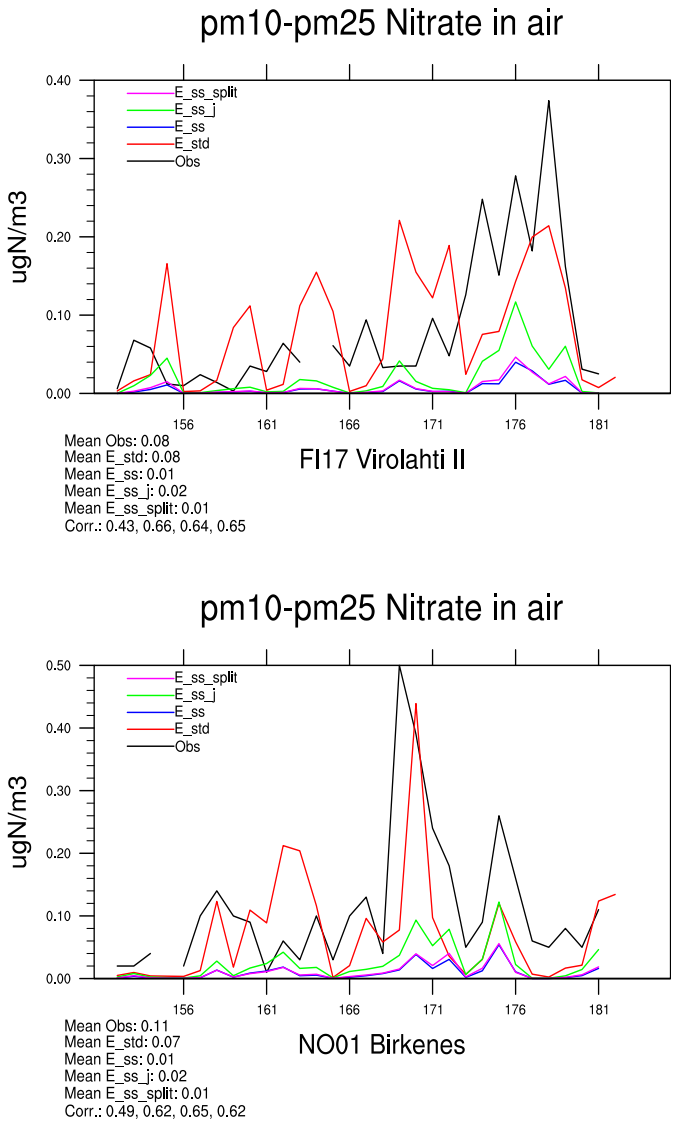

Figure 4.13: *Observed coarse nitrate and modelled coarse nitrate at FI17, upper panel and at NO01, lower panel, in June 2006. Both sensitivity model runs E_ss_j and E_ss_split are shown together with the standard run E_std and E_ss.*

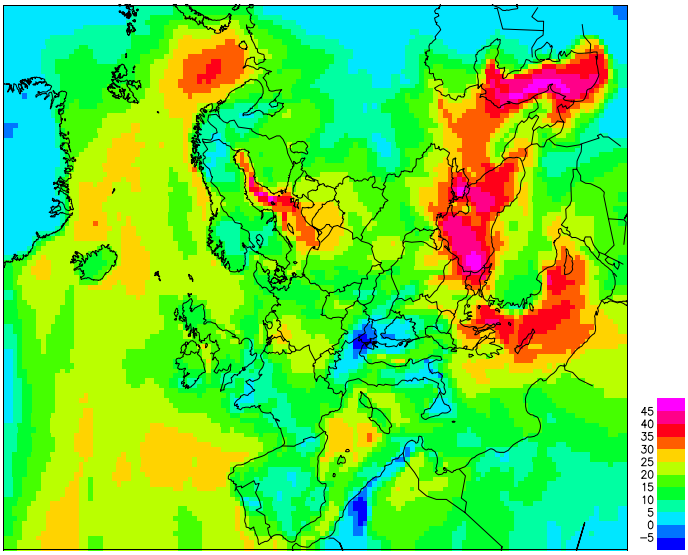

Figure 4.14: *The percent difference of coarse nitrate between E_ss_split and E_ss in June 2006.*

percent change between coarse nitrate in E_ss_split and E_ss in the whole EMEP area is shown. The monthly mean of coarse nitrate in June 2006 over the whole field is 0.04 μg(N) m^{-3} in E_ss_split. By using coarse sea-salt in 5 separate bins instead of assuming one coarse bin with one log-normal size distribution, there will be a switch towards smaller sizes of sea-salt in the coarse fraction. Separating coarse sea-salt in 5 different size bins does not enhance computational time significantly (5% increase in CPU time).

The sensitivity tests show that there are quite large differences in the amount of coarse nitrate with the different approaches of determining the size of coarse sea-salt. The effect on the correlation at the intensive measurement campaign stations is relatively low. The amount of coarse nitrate in the areas most affected is up to 400% percent higher in E_ss_j than in E_ss. In E_ss_split it is up to 49% higher.

4.3.4 Comparison to other work

Myhre et al. (2006) studied coarse nitrate formation on sea-salt for the year 2000 in a global chemistry-transport model, the Oslo CTM2. In that study the coarse ni-

trate formation on sea-salt follows a different approach, assuming an equilibrium between HNO_3 and NaCl and other ions. This method of assuming equilibrium of coarse aerosols probably causes an overestimation of coarse nitrate (Myhre et al., 2006). In Myhre et al. (2006) they calculate the annual mean of coarse nitrate, whereas in this thesis monthly means are calculated for June 2006 and January 2007 for E_ss. The average of these two months is used for comparison with Myhre et al. (2006) (Figure 4.15). This comparison reveals less coarse nitrate in E_ss than in the study of Myhre et al. (2006). It should also be kept in mind that the Myhre et al. (2006) study is done for a different year than this thesis, and that the annual mean is calculated in their study. The coarse mode in the Myhre et al. (2006) study starts at 1 μm in diameter while in the EMEP model the coarse mode starts from 2.5 μm, which will give less nitrate in this thesis. In E_ss_j which uses a size distribution for smaller aerosol there is still less coarse nitrate over land than in the study of Myhre et al. (2006), but the amount of coarse nitrate over the Mediterranean Sea is at some places up to 4 μg(NO_3^-) m^{-3}.

4.4 Coarse nitrate on dust and sea-salt

In this section the model run accounting for coarse nitrate formation on both dust and sea-salt is evaluated. In E_d_ss the same parameters for the size distribution and uptake coefficient of HNO_3 on dust and sea-salt are used as in E_d and E_ss. The parameters from E_ss_j have not been used here even if they give more coarse nitrate than E_ss, as with this choice the aerosols are in a size range closer to fine nitrate than coarse nitrate.

4.4.1 Day-to-day correlation

The correlation of coarse nitrate in E_d_ss is better than in E_std at all stations but NL11 in both June 2006 and January 2007, see Table 4.3. In June the correlation at most stations is mostly affected by the sea-salt implementation, the exceptions being ES17, CH02 and IT01, where dust also affects the correlation. In January 2007 the sea-salt implementation has a stronger influence than the dust implementation at all stations. At ES17, in June 2006, there is one peak of coarse nitrate that origins from the coarse nitrate formation on sea-salt, and one peak in the second half of June that origins form coarse nitrate formation on dust, as can be seen in Figure 4.16. The lack of continuous observations makes it uncertain if E_d_ss has the maxima of coarse nitrate at the right times.

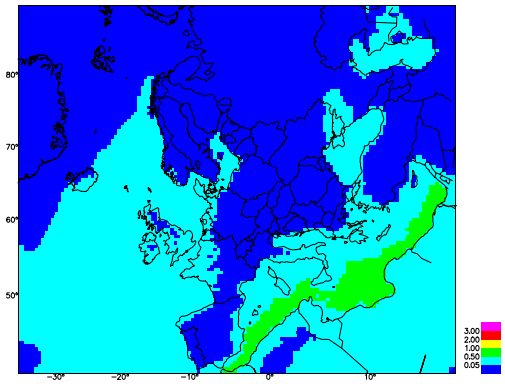

(a) *Average coarse nitrate in June plus January in E_ss*

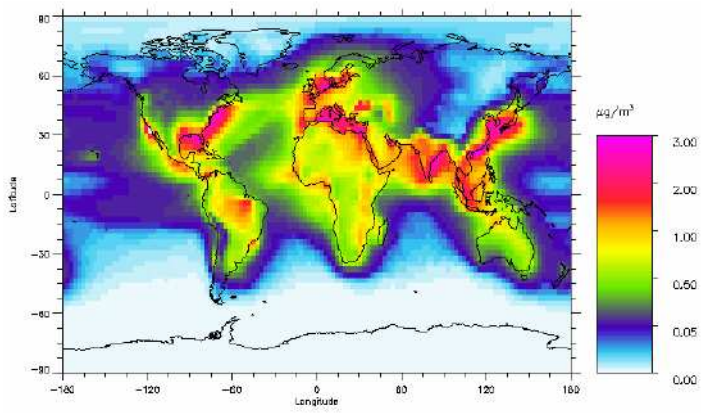

(b) *Annual mean of coarse nitrate in Myhre et al. (2006)*

Figure 4.15: *Coarse nitrate from this thesis in a) and figure 2 from Myhre et al. (2006) in b), both in* $\mu g(NO_3^-)\ m^{-3}$

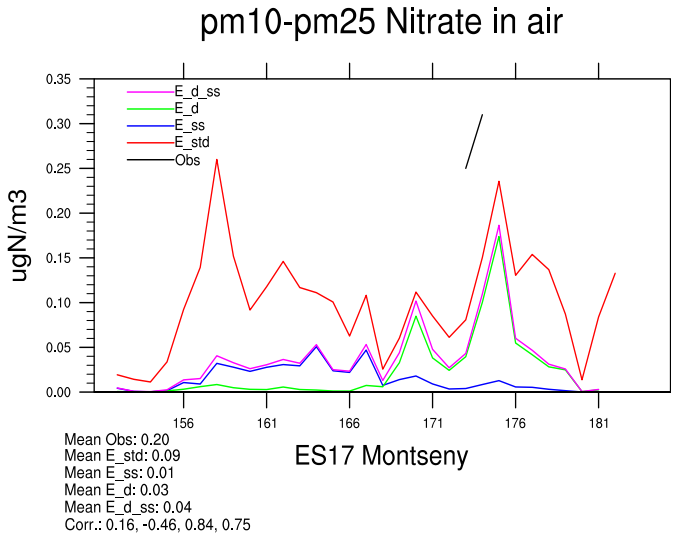

Figure 4.16: *Coarse nitrate at ES17 in June 2006, from the intensive measurement campaign. The difference between measured PM_{10} nitrate and $PM_{2.5}$ nitrate is compared to coarse nitrate in the EMEP model.*

It is encouraging to see that the correlation improves in the new parametrization with formation of coarse nitrate on both dust and sea-salt compared to the reference run at all stations in June 2006 and January 2007 (except NL11 in June 2006).

4.4.2 Amount of fine and coarse nitrate

Coarse nitrate in E_d_ss is lower than in the measurements from the intensive campaigns, both in June 2006 and in January 2007 (Table 4.3). Coarse nitrate forms almost exclusively over the ocean in E_d_ss and there are very low concentrations over land. Figure 4.17 shows the spatial variation of coarse nitrate in E_d_ss together with the observations of coarse nitrate. The amount of coarse nitrate is in the same range as in E_ss at the intensive measurement campaign stations. There are differences over the Mediterranean Sea and Northern Africa, the areas where formation of coarse nitrate on dust contributes to coarse nitrate in E_d_ss. There is less coarse nitrate in E_d_ss than in E_std as can be see from Figures 4.3 and 4.17, which are plotted with the same color scale for coarse nitrate.

Fine nitrate in E_d_ss is considerably lower than in the measurements from the intensive campaigns in June 2006. There is more fine nitrate in E_d_ss than in E_std both in June 2006 and in January 2007. This is probably caused by less formation of coarse nitrate in E_d_ss, and hence more HNO_3 to react with NH_3 to form fine nitrate. In January 2007 there is more fine nitrate in E_d_ss than in the measurement at some stations and less at other stations.

There is, in general, not enough coarse nitrate in E_d_ss compared to the intensive measurement stations, neither in June nor in January. In E_d_ss there is less coarse nitrate than in E_std, whereas more fine nitrate is revealed in E_d_ss than in E_std. Compared to measurements there is less fine nitrate in E_d_ss in June than in the measurements.

4.5 Coarse and fine nitrate on dust and sea-salt

In the evaluation of E_fine the focus will be on the differences between E_fine and E_d_ss. This is done to see if the formation of fine nitrate on fine dust and sea-salt has any effect on the partitioning of fine and coarse nitrate.

4.5.1 Day-to-day correlation

There are no significant changes in the correlation of fine nitrate by including formation of fine nitrate on fine dust and sea-salt in June 2006. In January there are changes in the correlation at some stations. The changes are highest at the northern coastal stations FI17 and NO01. At these stations correlation improves (see Table 4.2 for numbers and Figure 4.18 showing E_fine at FI17 in January 2007). FI17 and NO01 are stations where there is a lot of sea-salt, which probably explains the changes in the correlation.

The correlation of coarse nitrate is the same in E_fine as in E_d_ss in June. In January there are minor changes in the correlation of coarse nitrate between E_fine and E_d_ss at all stations. At some stations the correlation worsens and at others it improves. All the stations have a better correlation in E_fine than in E_std in both June and January, except NL11.

The correlation of coarse nitrate does not change significantly in neither of the

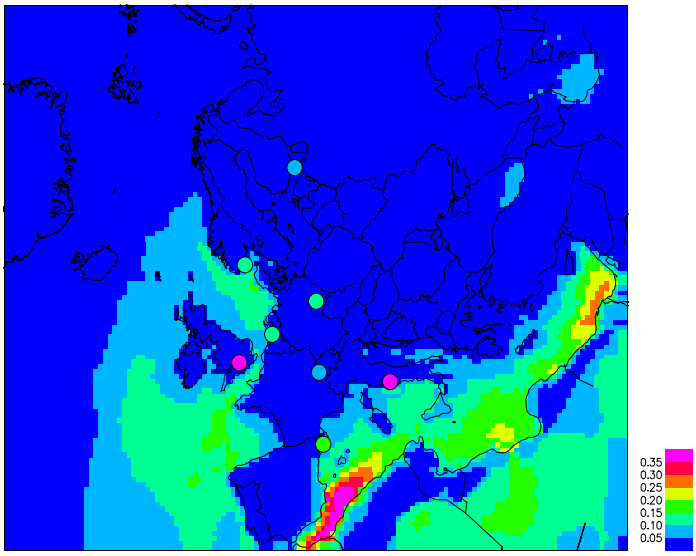

(a)

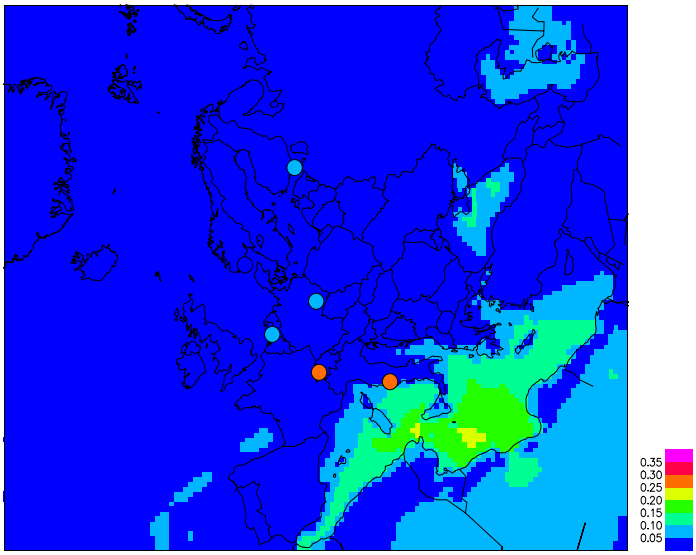

(b)

Figure 4.17: *Monthly mean of coarse nitrate in the model run with coarse nitrate formation on dust and sea-salt (E_d_ss) and observations of coarse nitrate at the stations from the intensive measurement period in a) June 2006 and b) January 2007. The bullets depict observations with the same color scale as the modelled field.*

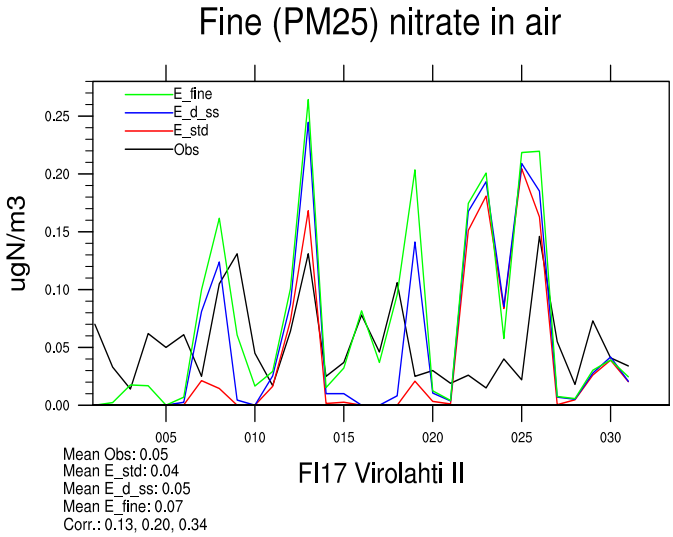

Figure 4.18: *Fine nitrate at FI17 in January 2007. E_fine is shown together with E_std and E_d_ss. E_fine improves the correlation at this station.*

two months studied here. While the correlation of fine nitrate improves at two stations in January, no significant changes are seen in June.

4.5.2 Amount of fine and coarse nitrate

Coarse nitrate is severely underestimated compared to the measurements with biases from -74% to -98% in both June and January. The result is similar to the result in E_d_ss with slightly smaller values at some stations.

Fine nitrate has lower values in E_fine than in the measurements in June at almost all stations. In January there is more fine nitrate in E_fine compared to measurements at some stations and less at others, see Table 4.2 for numbers. Compared to E_d_ss there is more fine nitrate in E_fine, especially at IE31 in June and at NO01 in January. The difference at the Norwegian station can be explained by less NH_3 in winter, and the inclusion of fine Na^+ will form fine nitrate as long as HNO_3 is available.

Including the formation of fine nitrate on dust and sea-salt yields more fine nitrate, especially in IE31 in June and NO01 in January. These two stations are stations relatively close to the coastline. There are no significant changes in coarse nitrate

in neither of the months.

4.5.3 Comparison to other work

Feng and Penner (2007) modelled nitrate in a global aerosol chemistry-transport model for the year 1997. They considered coarse and fine nitrate formation on both dust and sea-salt in a dynamical mass transfer calculation. In their study they assumed sea-salt to be 100% NaCl and an average Ca^{2+} content of 4.2% in dust, while in this thesis 5% Ca^{2+} content in dust is assumed. Their coarse mode nitrate is comprised of aerosols with diameter larger than 1.25 μm, which is lower than in the EMEP model where the coarse fraction are aerosols with diameter larger than 2.5 μm. In addition to coarse nitrate formation on calcite and dolomite in mineral dust, Feng and Penner (2007) considered coarse nitrate formation on K^+ and Na^+ on mineral dust. Monthly means from June 2006 and January 2007 in E_fine have lower amounts of coarse nitrate than in Feng and Penner (2007) (see Figure 4.19 to see the differences in January). One minor reason for the lower amount of coarse nitrate in E_fine is that smaller aerosols are included in the coarse fraction in Feng and Penner (2007), and they account for more reactions on dust. The differences might also come from different dust and sea-salt fields. In the fine nitrate field E_fine has also smaller values than in Feng and Penner (2007), but here the differences are smaller.

4.6 Gas-to-particle distribution in the new implementations

In this section measurements from the entire EMEP monitoring network are used, as in the evaluation of the gas-to-particle distribution in E_std. The periods evaluated are June 2006 and January 2007.

Modelled NH_3 is within a factor two at most stations, see Figures 4.20 and 4.21 where the result of E_fine are shown. At the Norwegian stations the new implementation underestimates NH_3 as in E_std. These Norwegian stations are probably affected by local sources as mentioned in the evaluation of NH_3 in E_std.There are hardly any changes in the model performance of NH_3 neither in June nor January in the model runs with the new parametrization.

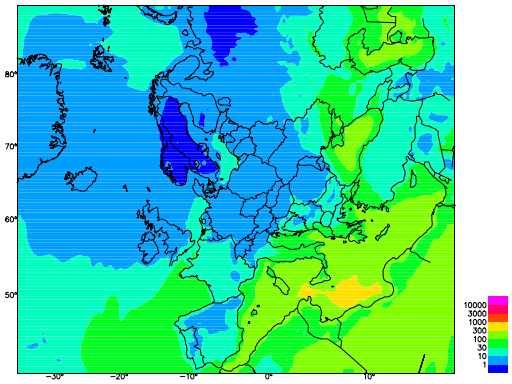

(a) *Monthly average of coarse nitrate in January 2007 in E_fine*

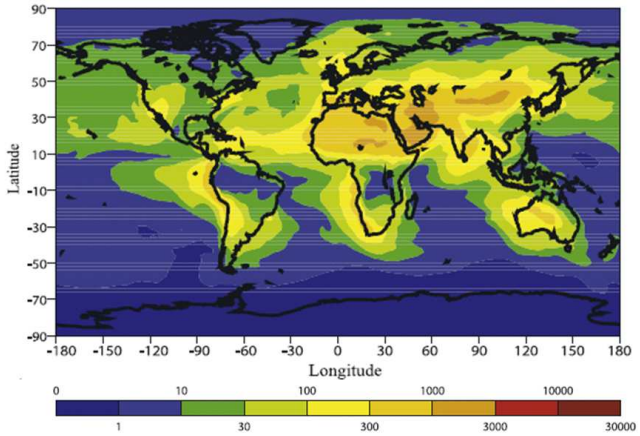

(b) *Monthly average coarse nitrate January 1997, figure 2 from Feng and Penner (2007)*

Figure 4.19: *Coarse nitrate in this study a) and from Feng and Penner (2007) in b). Both Figures shows coarse nitrate in pptv NO_3^-. Coarse nitrate in E_fine are > 2.5 μm in diameter, while in Feng and Penner (2007), coarse nitrate are > 1.25 μm in diameter.*

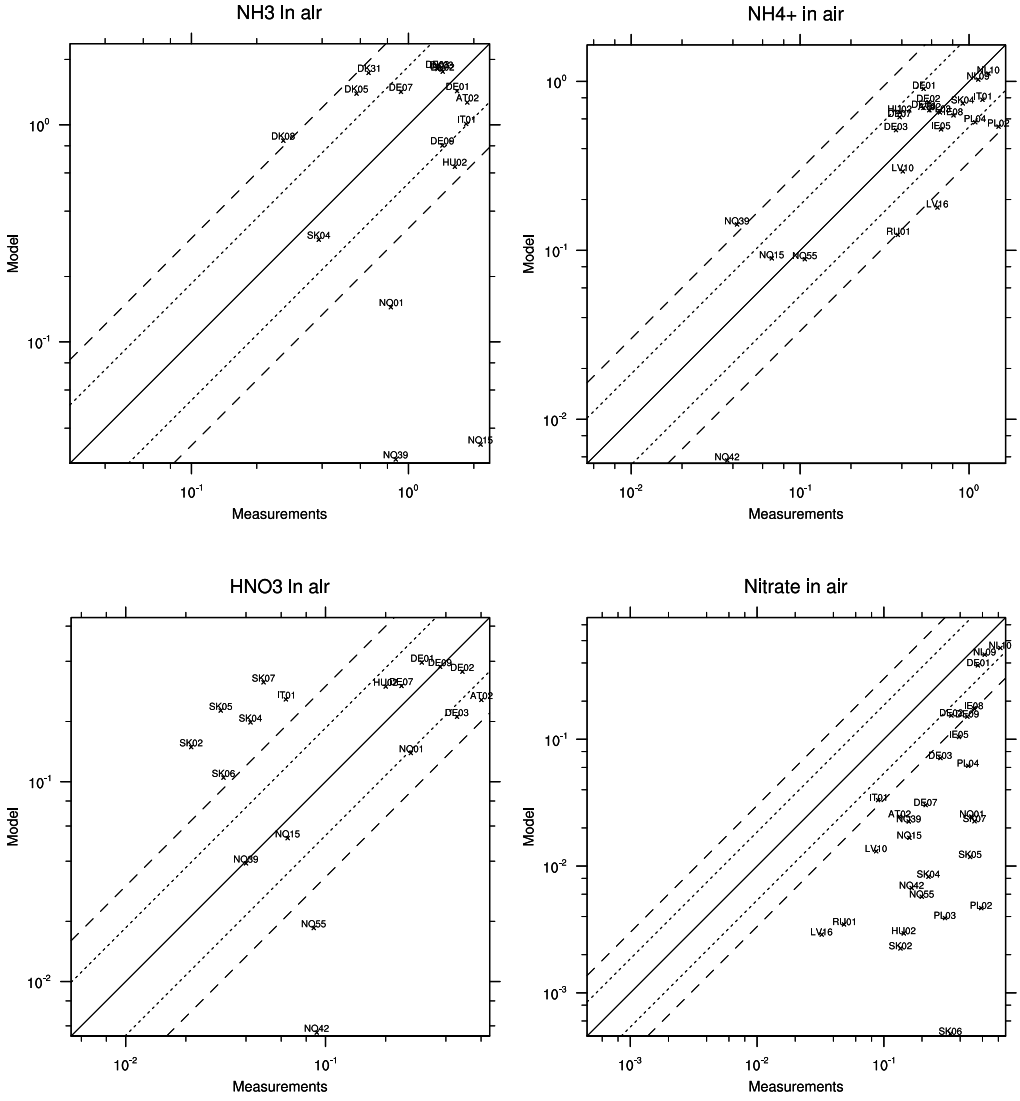

Figure 4.20: *Comparison of modelled NH_3, NH_4^+, HNO_3 and particulate nitrate in E_std with measurements from the standard EMEP network in June 2006. Measurement and model averages over the stations together with correlations are given in Table 4.1.*

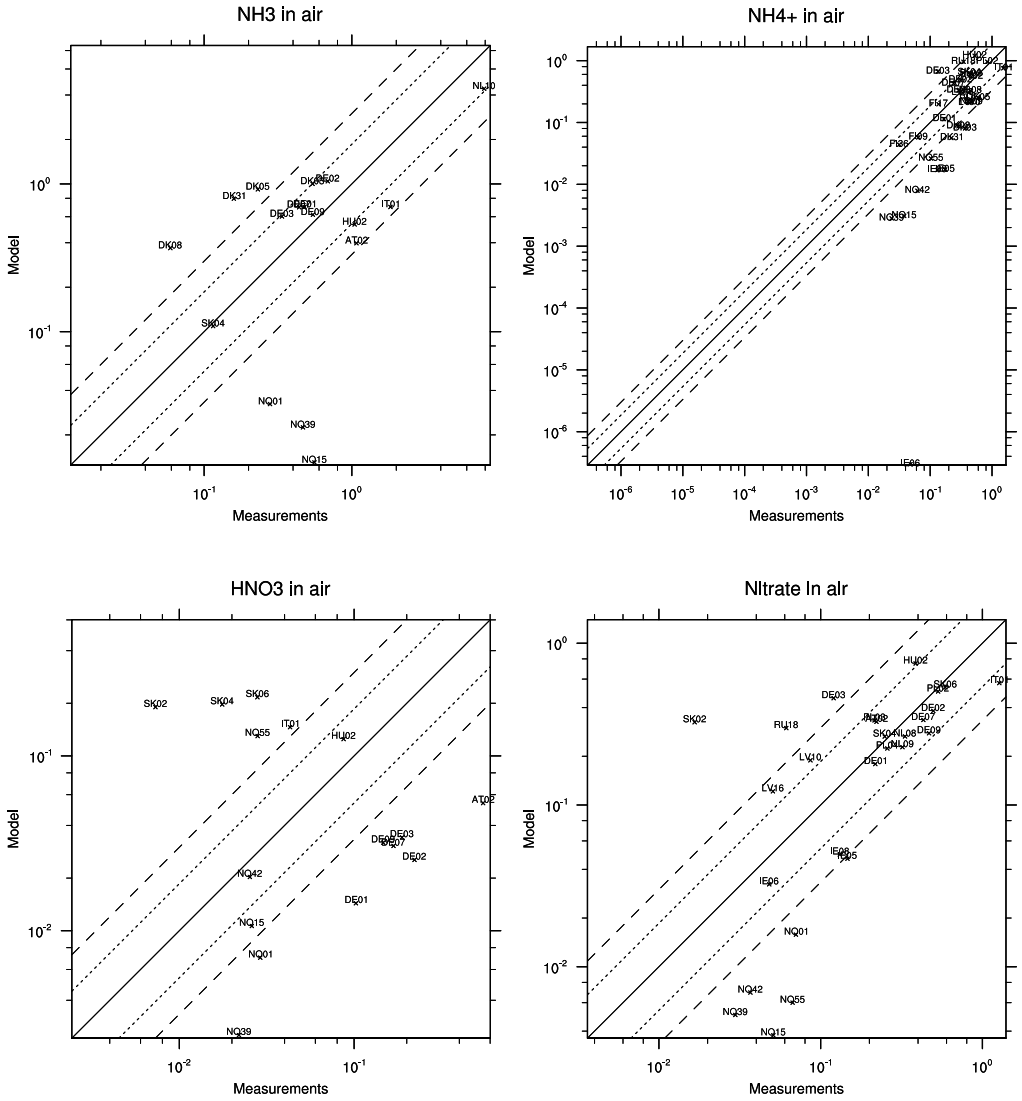

Figure 4.21: *Comparison of modelled NH_3, NH_4^+, HNO_3 and particulate nitrate in E_fine and measurements from the standard EMEP network in January 2007. Numbers for the measurement average over the stations, bias and correlation are given in Table 4.1.*

In general, small changes are seen in modelled values of NH_4^+ at the stations. In E_std the monthly modelled mean in June was 0.55 μg(N) m^{-3}, which has changed to 0.58 μg(N) m^{-3} and 0.54 μg(N) m^{-3} in E_d_ss and E_fine, respectively. In January there is a comparable change, except that one station in E_fine disengages from the other model runs, with IE06 being severely underestimated (see Figure 4.21).

There is more nitric acid in E_d_ss and E_fine than in E_std in both June and January (Table 4.1). The smaller coarse nitrate formation in the new parametrization can probably explain the higher amount of HNO_3 in these model runs.

In June there is a mean value of 0.08 μg(N) m^{-3} particulate nitrate in E_d_ss and E_fine, while in E_std the mean value was 0.12 μg(N) m^{-3}. In January the modelled mean of particulate nitrate is 0.25, while in E_d_ss and E_std the values are 0.23 μg(N) m^{-3} and 0.20 μg(N) m^{-3}, respectively. When comparing particulate nitrate in Figure 4.2 and 4.21 the differences between E_std and E_fine seem to be caused by more modelled nitrate at the Irish stations.

There are no significant changes between the different model runs in the gas-to-particle distribution. In the new parametrization there is more HNO_3 probably due to less coarse nitrate formation. In the evaluation of nitrate in this section total nitrate aerosols are evaluated. This evaluation shows that the model has similar results against measurements with the new parametrization as with the old parametrization, even if the evaluation of coarse nitrate revealed a high underestimation of coarse nitrate against measurements. This shows how important it is to evaluate model results against measurements of fine and coarse nitrate, in order to see how the model performs in terms of nitrate.

4.7 Spatial correlation

Scatter plots of measured coarse nitrate and modelled coarse nitrate in E_d, E_ss, E_d_ss and E_std in June 2006 and January 2007 are shown in Figure 4.22. In June the spatial correlation is the same in E_d_ss and E_std (r=0.79); it is worse in E_ss and E_d than in E_d_ss. The spatial correlations are higher in January than in June in all model runs. In January the spatial correlation is slightly worse in the new implementation than in the standard run. The implementation with the best spatial correlation in January is E_d.

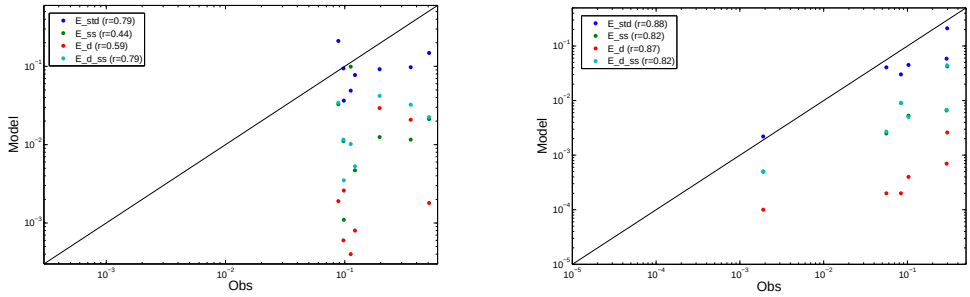

(a) June 2006 (b) January 2007

Figure 4.22: *The spatial correlation of coarse nitrate in E_std, E_ss, E_d and E_d_ss in a) June 2006 and b) January 2007.*

The spatial correlation does not change significantly with the new parametrization. It is still relatively high even if the model forms too small amounts of coarse nitrate in both June and January. The spatial correlations of E_d and E_ss are worse than for E_std and E_d_ss, which is expected as only one of the formation pathways of coarse nitrate is implemented here. The fact that the same values of spatial correlation are found in E_std and E_d_ss shows that both parametrizations are driven by HNO_3, and high values of HNO_3 give high values of coarse nitrate. That the new parametrization does not give a better spatial correlation may imply that the spatial correlation of dust and NaCl is not good enough to give an improvement in the model. The day-to-day correlation, however, becomes better.

Chapter 5

Summary and conclusion

In this thesis a new parametrization of coarse nitrate on mineral dust and sea-salt is implemented in the Unified EMEP model. The formation of coarse nitrate on dust involves the reactions between HNO_3 and calcite and dolomite, the most reactive part of mineral dust towards HNO_3. The formation of coarse nitrate on sea-salt involves the reaction between HNO_3 and NaCl. A full heterogeneous reaction in the forward direction is assumed for both mineral dust and sea-salt. The implementations of coarse nitrate formation on dust and sea-salt are tested separately and in combination to allow for an evaluation of their individual and total effects on the model performance. Finally a model run including, in addition, the formation of fine nitrate on sea-salt and dust is performed. Several test runs are done to assess the sensitivity of the implementations to various parameters.

The model results are compared to measurements of nitrate aerosols from the intensive measurement campaigns in June 2006 and January 2007, as these are the only sets of measurements that separate fine and coarse aerosols. The aim of this thesis was to examine if the EMEP model gives a better reproduction of coarse nitrate formation by explicitly including the uptake of HNO_3 on coarse sea-salt and dust.

The results from this thesis can be summarized as follows:

- The new parametrization of coarse nitrate on dust and sea-salt improves the temporal correlation at all measurement stations from the intensive measurement campaigns, except at the Dutch station NL11 in June 2006.
- Coarse nitrate in the new parametrization is severely underestimated at the

measurement stations. However, it should be noted that the selection of stations can affect the results of the evaluation. In June and January the evaluation of coarse Ca^{2+} and Na^{+} reveals a severe underestimation, while the yearly evaluation against measurements of total aerosol (i.e. including all sizes) from the standard EMEP monitoring network shows less severe disagreement (-51% for total Ca^{2+}, and +25% for total Na^{+}). This suggests that either the months of June 2006 and January 2007 are not well modelled or the selected stations are not sufficiently representative for the precursors sea-salt and dust.

- There are only two months of intensive measurements and thus very few observations separating coarse and fine nitrate. Indeed, at some stations there are no continuous measurements even in the two months of the intensive campaigns. This is not sufficient for a thorough evaluation.

- The sensitivity of the different parameters in the implementation of coarse nitrate on dust and sea-salt was tested. The uptake coefficient of HNO_3 on dust was tested, together with the Ca^{2+} content in dust and the size distribution of sea-salt. Neither of these sensitivity studies could explain the severe underestimation of coarse nitrate in the model results with the new parametrization.

- The inclusion of fine nitrate formation on fine dust and sea-salt does not change the model results of coarse nitrate significantly. There are some changes in fine nitrate in the model, yielding more fine nitrate at some stations.

- The comparison with other model studies of coarse nitrate formation on dust and sea-salt reveals a relatively small formation of coarse nitrate in this study. Part of the differences is due to the different methods used in the other studies. Another reason is the assumption of a higher Ca^{2+} content in dust, and possibly more dust in the model. The model-measurement comparisons found in the other studies focus on total nitrate only, which does not give a direct measure of how the coarse nitrate parametrization performs.

In the future an alternative method of implementing coarse nitrate on dust and sea-salt could be tried in the EMEP Unified Model, as the present method yields a severe underestimation. The equilibrium method is one possible approach, and the EQSAM module could be used for this purpose. However, it should be taken

into account that formation of coarse nitrate does not reach equilibrium within the 20-minute chemical time step in the EMEP model. It is also desirable to get more measurements of coarse and fine nitrate to allow for a more comprehensive evaluation of nitrate in the EMEP model. If possible one should also attempt to implement a chemical speciation of dust in the EMEP model, as the Ca^{2+} content in dust represents a major uncertainty in the implementation of coarse nitrate on dust.

Given the rather high uncertainties regarding the formation of nitrate and its life cycle in the Earth system, combined with the increasing relative importance of nitrate aerosols to the ecosystem, human health, and climate, it is clear that improvements in the modeling of nitrate in particular and the nitrogen cycle in general should be among the research priorities in the years to come.

Bibliography

Bauer, S. E., D. Koch, N. Unger, S. M. Metzger, D. T. Shindell, and D. G. Streets (2007). Nitrate aerosols today and in 2030: A global simulation including aerosols and tropospheric ozone. *Atmos.Chem.Phys.,7 7*, 5043–5059.

Berge, E. and H. A. Jakobsen (1998). A regional scale multi-layer model fro the calculation of long-term transport and deposition of air pollution in Europe. *Tellus 50*, 205–223.

Bott, A. (1989a). A positive definite advection scheme obtained by nonlinear renormalization of the advective fluxes. *Mon. Weath. Rev. 117*, 1006–1015.

Bott, A. (1989b). Reply. *Mon. Weath. Rev 117*, 2633–2636.

Capaldo, K. P., C. Pilinis, and S. N. Pandis (2000). A computationally efficient hybrid approach for dynamic gas/aerosol transfer in air quality models. *Atmospheric Environment 34*, 3617–3627.

Daizhou, Z., S. Guangyu, I. Yasunobu, H. Min, and Z. Jiaye (2005, December). Anthropogenic calcium particles observed in Bejing and Qingdao, China. *Water, Air and Soil Pollution: Focus 5*, 261–276.

Dentener, F. (1993). *Heterogeneous chemistry in the troposphere*. Ph. D. thesis, University of Utrecht.

Dentener, F. J., G. R. Carmichael, Y. Zhang, J. Lelieveld, and P. J. Crutzen (1996, October). Role of mineral aerosol as a reactive surface in the global troposphere. *Journal of geophysical research, 101 101*(D17), 22869–22889.

Dollard, G. J., D. H. F. Atkins, T. J. Davies, and C. Healy (1987, April). Concentration and dry deposition of nitric acid. *Nature 326*.

Fagerli, H. and W. Aas (2008). Intensive measurement periods in: Transboundary acidification, eutrophication and ground level control in Europe, EMEP status report 1/2008, p.105-122. Technical report, The Norwegian Meteorological Institute, Oslo, Norway.

Fagerli, H., D. Simpson, and S. Tsyro (2004). Unified EMEP model: Updates in: Transboundary acidification, eutrophication and ground level control in Europe,EMEP status report 1/2004, p.11-18. Technical report, The Norwegian Meteorological Institute, Oslo, Norway.

Feng, Y. and J. E. Penner (2007). Global modeling of nitrate and ammonium: Interaction of aerosols and tropospheric chemistry. *Journal of geophysical research 112*, D01304.

Fenter, F. F., F. Caloz, and M. J. Rossi (1995). Experimental evidence for the efficient "dry deposition" of nitric acid on calcite. *Atmospheric Environment 29*(22), 3365–3372.

Goodman, A. L., G. M. Underwood, and V. H. Grassian (2000, December). A laboratory study of the heterogeneousre action of nitric acid on calcium carbonate particles. *Journal of geophysical research 105*(D23), 29053–29064.

Grini, A., G. Myhre, C. S. Zender, and I. S. A. Isaksen (2005). Model simulation of dust sources and transport in the global atmosphere: Effect of soil erodibility and wind speed variability. *Journal of Geophysical Research 110*, D02205.

Guimbard, C., F. Arens, L. Gutzwiller, H. W. Gäggeler, and M. Ammann (2002). Uptake of HNO_3 to deliquescent sea-salt particles: A study using the short-lived radioactive isotope tracer ^{13}N. *Atmospheric chemistry and physics 2*, 249–257.

Hanisch, F. and J. N. Crowley (2001). The heterogeneous reactivity of gaseous nitric acid on authentic mineral dust samples, and on individual mineral and clay mineral components. *Physical Chemistry Chemical Physics 3*, 2474–2482.

Hodzic, A., B. Bessagnet, and R. Vautard (2006). A model evaluation of coarse-mode nitrate heterogeneous formation on dust particles. *Atmospheric Environment 40*, 4158–4171.

Huebert, B. J. and C. H. Robert (1985, February). The Dry Deposition of Nitric-Acid to Grass. *Journal of geophysical research 90*(D1), 2085–2090.

Husar, B. H. (2004). Intercontinental transport of dust: Historical and recent observational evidence. In A. Stohl (Ed.), *Intercontinental transport of air pollution*. Springer.

IPCC 2001: Penner, J. E., M. Andreae, H. Annegarn, L. Barrie, J. Feichter, D. Hegg, A. Jayaraman, R. Leaitch, D. Murphy, J. Nganga, and G. Pitari (2001). Aerosols, their Direct and Indirect Effects. *Climate Change 2001: The Scientific Basis. Contribution of Working Group I to the Third Assessment Report of the Intergovernmental Panel on Climate Change [Houghton, J.T.,Y. Ding, D.J. Griggs, M. Noguer, P.J. van der Linden, X. Dai, K. Maskell, and C.A. Johnson (eds.)]. Cambridge University Press, Cambridge, United Kingdom and New York, NY, USA, 881pp.*, 297.

IPCC 2007: Climate Change 2007: Synthesis Report. Contribution of Working Groups I, II and III to the Fourth Assessment Report of the Intergovernmental Panel on Climate Change [Core Writing Team, Pachauri, R.K and Reisinger, A. (eds.)]. IPCC, Geneva, Switzerland, 104 pp.

Jacob, Daniel, J. (1999). *Introduction to atmospheric chemistry*. Princeton University Press.

Jaenicke, R. (1988). *Numerical Data and Functional Relationships in Science and Technology*. Springer, Berlin.

Jonson, J., L. Tarrasón, and J. Sundet (1999). Calculation of ozone and other pollutants of the summer 1996. *Environ. Manag. Health 10*, 245–257.

Kelly, J. T. and A. S. Wexler (2005, June). Thermodynamics of carbonates and hydrates related to heterogeneous reactions involving mineral aerosol. *Journal of geophysical research 110*, DI1201.

Krueger, B. J., V. H. Grassian, J. P. Cowin, and A. Laskin (2004). Heterogeneous chemistry of individual mineral dust particles from different dust source regions: the importance of particle mineralogy. *Atmospheric Environment 38*, 6253–6261.

Krueger, B. J., V. H. Grassian, J. P. Cowin, and A. Laskin (2005). Erratum to "Heterogeneous chemistry of individual mineral dust particles from different dust source regions: the importance of particle mineralogy"[atmos. environ. 38 (36) (2004) page 6253-6261]. *Atmospheric Environment 39*, 395.

Krupa, S. V. (2003). Effects of atmospheric ammonia (NH_3 on terrestrial vegetation: a review). *Environmantal Pollution 124*, 179–221.

Liao, H., P. J. Adams, S. H. Chung, J. H. Seinfeld, L. J. Mickley, and D. J. Jacob (2003). Interaction between tropospheric chemistry and aerosols in a unified general circulation model. *Journal of geophysical research, 108 108*(D1), 4001.

Liu, Y., J. P. Cain, H. Wang, and A. Laskin (2007). Kinetic study of heterogeneous reation of deliquesced NaCl particles with gaseous HNO_3 using particle-on-substrate stagnation flow reator approach. *J.Phys.Chem 111*(40), 10026–10043.

Liu, Y., E. R. Gibson, J. P. Cain, H. Wang, V. H. Grassian, and A. Laskin (2008). Kinetics of heterogeneous reaction of $CaCO_3$ particles with gaseous HNO_3 over a wide range of humidity. *J. Phys. Chem 112*, 1561–1571.

Loon, M., L. Tarrasón, and M. Posch (2005). Modelling base cations in Europe. Technical report, EMEP MSC-W, http://emep.int/publ/reports/2005/emep_technical_2_2005.pdf.

Loÿe-Pilot, M. D., J. M. Martin, and J. Morelli (1986, May). Influence of Saharan dust on the rain acidity and atmospheric input to the Mediterranean. *Nature 321*(22).

Mamane, Y. and J. Gottlieb (1992). Nitrate formation on sea-salt and mineral particles–a single particle approach. *Atmospheric environment 26A*(9), 1763–1769.

Marticorena, B. and G. Bergametti (1995). Modeling the atmospheric dust cycle: 1. Design of a soli-derived dust emission scheme. *Journal of geophysical research 100*(D8), 16415–16430.

Martin, S. T., H. M. Hung, R. J. Park, D. J. Jacob, R. J. D. Spurr, K. V. Chance, and M. Chin (2004). Effects of the physical state of tropospheric ammonium-sulfate-nitrate particles on global aerosol direct radiative forcing. *Atmos. Chem. Phys. 4*, 183–214.

Meng, Z. and J. H. Seinfeld (1996). Time scale to achieve atmospheric gas-aerosol equilibrium for volatile species. *Atmospheric Environment 30*, 2889–2900.

Metzger, S. M., F. J. Dentener, J. Lelieveld, and S. N. Pandis (2002). Gas/aerosol partitioning 1. A computionally efficient model. *Journal of geophysical research D16*(107), 4312.

Meyers, T. P., B. J. Huebert, and B. B. Hicks (1989). HNO_3 deposition to a deciduous forest. *Boundary-Layer Meteorology 49*(4), 395–410.

Monahan, E. C., D. E. Spiel, and K. L. Davidson (1986). *A model of marine aerosol generation via white caps and wave disruption*, Chapter pages 167-193, pp. 167–193. Dordrecht: Reidel, The Netherlands.

Muller, H., G. Kramm, F. Meixner, G. J. Dollard, D. Fowler, and M. Possanzini (1993). Determination of HNO_3 Dry Deposition by Modified Bowen-Ratio and Aerodynamic Profile Techniques. *Tellus Series B - Chemical and Physical Meteorology 45*(4), 346–367.

Myhre, G., A. Grini, and S. Metzger (2006). Modelling of nitrate and ammonium-containing aerosols in presence of sea salt. *Atmos. Chem. Phys. 6*, 4809–4821.

Mårtensson, E. M., E. D. Nilsson, G. de Leeuw, L. H. Cohen, and H. C. Hansson (2003, May). Laboratory simulations and parametrization of the primary marine aerosol production. *Journal of geophysical research 108*(D9), 4297.

O'Dowd, C. D., M. H. Smith, I. E. Consterdine, and J. A. Lowe (1997). Marine aerosol, sea-salt, and the marine sulphur cycle: A short review. *Atmospheric environment 31*(1), 73–80.

Pandis, S. S. and J. H. Seinfeld (1998). *Atmospheric chemistry and physics From air pollution to climate change*. wiley-interscience publication.

Pryor, S. C., M. Callagher, H. Sieverin, S. E. Larsen, R. J. Barthelmie, F. Birsan, E. Nemitz, J. Rinne, M. Kulmala, T. Grönholm, R. Taipale, and T. Vesala (2008). A review of measurement and modelling results of particle atmosphere-surface exchange. *Tellus 60B*, 42–75.

Putaud, J.-P., F. Raes, R. Van Dingenen, E. Brüggemann, M.-C. Facchini, S. Decesari, S. Fuzzi, R. Gehrig, C. Hüglin, P. Laj, G. Lorbeer, M. W., N. Mihalopoulos, K. Müller, X. Querol, S. Rodriguez, J. Schneider, G. Spindler, H. ten Brink, K. Tørseth, and A. Wiedensohler (2004). A European aerosol phenomenology 2:chemical characteristics of particulate matter at kerbside, urban, rural and background sites in Europe. *Atmospheric environment 38*, 2579–2595.

Saul, T. D., M. P. Tolocka, and M. V. Johnston (2006). Reactive uptake of nitric acid onto sodium chloride aerosols across a wide range of relative humidities. *journal of physical chemstry 110*, 7614–7620.

Schaap, M., G. Spindler, M. Schulz, K. Acker, W. Maenhaut, A. Berner, W. Wieprecht, M. Streit, K. Müller, E. Brüggemann, X. Chi, J.-P. Putaud, R. Hitzenberger, H. Puxbaum, U. Baltensperger, and H. ten Brink (2004). Artefacts in the sampling of nitrate in the "INTERCOMP" campaigns of EUROTRAC-AEROSOL. *Atmospheric Environment 38*, 6487–6496.

Simpson, D. (1995). Biogenic emissions in Europe 2: Implications for ozone control srategies. *Journal of geophysical research 100*, 22891–22906.

Simpson, D., H. Fagerli, J. E. Jonson, S. Tsyro, P. Wind, and J. P. Tuovinen (2003). The EMEP Unified Eulerian Model. Model description.EMEP MSC-W Report 1/2003. Technical report, The Norwegian Meteorological Institute, Oslo, Norway.

Stemmler, K., C. Vlasenko, A. Guimbaud, and M. Ammann (2008). The effect of fatty acid surfactants on the uptake of nitric acid to deliquesced NaCl aerosol. *Atmospheric chemistry and physics 8*, 5127–5141.

Tolocka, M. P., T. D. Saul, and M. Johnston (2004, February). Reactive uptake of nitric acid into aqueous sodium chloride droplets using real-time single-particle mass spectrometry. *J. Phys. Chem. 108*, 2659–2665.

Tsyro, S. (2008). Regional Model for Formation, Dynamics and Long-range Transport of Atmospheric Aerosol. *Russian meteorology and hydrology 33*(2), 82–90.

Tsyro, S. and W. Aas (2008). Comparison of model results with data from the emep intensive measurements in: Transboundary particulate matter in Europe Status report 4/2008, p.73-89. Technical report, The Norwegian Meteorological Institute, Oslo, Norway.

Umann, B., F. Arnold, C. Schaal, M. Hanke, J. Uecker, H. Aufmhoff, Y. Balkanski, and R. Van Dingenen (2005). Interaction of mineral dust with gas phase nitric acid and sulfur dioxide during the MINATROC II field campaign: First estimate of the uptake coefficient γ_{HNO_3} from atmospheric data. *Journal of Geophysical Research 110*, D22306.

Usher, C. R., A. E. Michel, and V. H. Grassian (2003). Reactions on mineral dust. *Chemical Reviews 103*, 4883–4940.

Vestreng, V., L. Ntziachristos, A. Semb, S. Reis, I. S. A. Isaksen, and L. Tarrasón (2009). Evolution of NO_x emissions in Europe with focus on road transport control measures. *Atmos. Chem. Phys 9*, 1503–1520.

Vlasenko, A., S. Sjogren, E. Weingartner, K. Stemmler, H. W. Gäggeler, and M. Ammann (2006). Effect of humidity on nitric acid uptake to mineral dust aerosol particles. *Atmospheric chemistry an physics 6*, 2147–2160.

Wallace, John., M. and V. Hobbs, Peter (2006). *Atmospheric Science An Introductory Survey*, Chapter 5, pp. 153–198. Academic Press.

Wesely, M. L. (1989). Parametrization of surface resistances to gaseous dry deposition in regional scale numerical models. *Atmospheric Environment 23*, 1293–1304.

WHO: Joint WHO/Convention Task Force on the Health Aspects of Air Pollution (2006). Health risks of particulate matter from long-range transboundary air pollution. Copenhagen, WHO Regional Office for Europe. (http://www.euro.who.int/document/E88189.pdf, accessed 27 July 2009).

Wu, P.-M. and K. Okada (1994, january). Nature of coarse nitrate particles in the atmosphere -a single particle approach. *Atmospheric Environment 28*(12), 2053–2060.

Zender, C. S., H. Bian, and D. Newman (2003). Mineral dust entrainment and deposition (DEAD) model: Description and 1990s dust climatology. *Journal of geophysical researc 108*(D14), 4416.